

This is a repository copy of *Hematopoietic stem cells retain functional potential and molecular identity in hibernation cultures*.

White Rose Research Online URL for this paper:

<https://eprints.whiterose.ac.uk/172953/>

Version: Accepted Version

Article:

Oedekoven, Caroline A, Belmonte, Miriam, Bode, Daniel et al. (12 more authors) (2021) Hematopoietic stem cells retain functional potential and molecular identity in hibernation cultures. *Stem Cell Reports*. pp. 1614-1628. ISSN 2213-6711

<https://doi.org/10.1016/j.stemcr.2021.04.002>

Reuse

Items deposited in White Rose Research Online are protected by copyright, with all rights reserved unless indicated otherwise. They may be downloaded and/or printed for private study, or other acts as permitted by national copyright laws. The publisher or other rights holders may allow further reproduction and re-use of the full text version. This is indicated by the licence information on the White Rose Research Online record for the item.

Takedown

If you consider content in White Rose Research Online to be in breach of UK law, please notify us by emailing eprints@whiterose.ac.uk including the URL of the record and the reason for the withdrawal request.

1 **Hematopoietic stem cells retain functional potential and molecular identity**
2 **in hibernation cultures**

3

4 *Caroline A. Oedekoven^{1,2}, *Miriam Belmonte^{1,2}, Daniel Bode^{1,2}, Fiona K. Hamey^{1,2}, Mairi S
5 Shepherd^{1,2}, James Lok Chi Che^{1,2}, Grace Boyd³, Craig McDonald^{1,2}, Serena Belluschi^{1,2},
6 Evangelia Diamanti^{1,2}, Hugo P. Bastos^{1,2}, Katherine Bridge³, Berthold Göttgens^{1,2}, †Elisa
7 Laurenti^{1,2}, and †David G. Kent^{1,2,3}

8

9 ¹Wellcome MRC Cambridge Stem Cell Institute, University of Cambridge, Hills Road,
10 Cambridge, CB2 0XY, United Kingdom

11 ²Department of Haematology, University of Cambridge, CB2 0XY, United Kingdom

12 ³York Biomedical Research Institute, Department of Biology, University of York, York, YO10
13 5DD, United Kingdom

14 *These authors contributed equally to the study

15 †These authors contributed equally to the study

16

17 **Address correspondence:**

18 David G. Kent, York Biomedical Research Institute, Department of Biology, University of
19 York, York, YO10 5DD

20 Telephone (+44) 1904 328847

21 E-mail david.kent@york.ac.uk

22

23

24 **Summary**

25 Advances in the isolation and gene expression profiling of single hematopoietic stem cells
26 (HSCs) have permitted in-depth resolution of their molecular program. However, long-term
27 HSCs can only be isolated to near purity from adult mouse bone marrow, thereby precluding
28 studies of their molecular program in different physiological states. Here, we describe a
29 powerful 7-day HSC hibernation culture system that maintains HSCs as single cells in the
30 absence of a physical niche. Single hibernating HSCs retain full functional potential compared
31 to freshly isolated HSCs with respect to colony forming capacity and transplantation into
32 primary and secondary recipients. Comparison of hibernating HSC molecular profiles to their
33 freshly isolated counterparts showed a striking degree of molecular similarity, further
34 resolving the core molecular machinery of HSC self-renewal while also identifying key factors
35 that are potentially dispensable for HSC function including members of the AP1 complex (*Jun*,
36 *Fos*, and *Ncor2*), *Sult1a1* and *Cish*. Finally, we provide evidence that hibernating mouse HSCs
37 can be transduced without compromising their self-renewal activity and demonstrate the
38 applicability of hibernation cultures to human HSCs.

39
40
41
42
43
44
45
46
47

48 **Introduction**

49 The blood-forming system is sustained by a rare subset of hematopoietic stem cells (HSCs)
50 with the potential to differentiate into all mature blood cell types and to create equally potent
51 daughter HSCs to maintain tissue homeostasis (Doulatov *et al.*, 2012; Eaves, 2015; Laurenti
52 and Göttgens, 2018; Ganuza *et al.*, 2020). As the seed cells for the blood system, their clinical
53 potential for cellular therapies is vast and the need to understand their molecular program in
54 different physiological states is critical for their therapeutic application. Recently, cell culture
55 conditions have been reported to produce large numbers of functional mouse and human
56 HSCs (Fares *et al.*, 2017; Wilkinson *et al.*, 2019), but in all cases, the substantial majority of
57 cells produced are non-HSCs (Gundry *et al.*, 2016; Bak, Dever and Porteus, 2018; Shepherd
58 and Kent, 2019; Wagenblast *et al.*, 2019).

59 In the absence of robust purification strategies for functional HSCs in culture, it becomes
60 virtually impossible to study the molecular profile of HSCs removed from their *in vivo*
61 microenvironment. Previous studies have highlighted the potential for retaining LT-HSC
62 function in cultures with low amounts of proliferation in the absence of excessive cytokine-
63 induced signalling (Yamazaki *et al.*, 2006, 2009; Kobayashi *et al.*, 2019), although these
64 cultures were still predominantly non-HSCs. An *in vitro* system that could retain highly
65 purified single HSCs would offer the potential to molecularly profile niche-independent HSCs
66 and to resolve the essential components of self-renewal *in vitro*.

67 Here, we describe such a system, demonstrating that fully functional mouse LT-HSCs can be
68 maintained in minimal cytokine conditions over a period of 7 days without undergoing cell
69 division. This novel cell culture system preserves the core features of HSCs including the speed
70 of quiescence exit, subsequent cell cycle kinetics, mature cell production, and HSC self-
71 renewal activity in serial transplantation assays. The functional properties of these
72 hibernating HSCs are virtually indistinguishable from freshly isolated HSCs and molecular
73 profiling by single cell RNA-sequencing shows a high degree of overlap with freshly isolated
74 HSCs, but also reveals a number of molecular changes that identify genes potentially
75 dispensable for retaining HSC function.

76

77

78

79 **Results**

80 **Single LT-HSCs can retain multipotency *in vitro* under minimal cytokine stimulation**

81 Previous studies suggested that SCF and TPO are essential for HSC self-renewal and
82 proliferation, but potentially dispensable for stem cell maintenance (Yamazaki *et al.*, 2006,
83 2009; De Graaf and Metcalf, 2011). A number of studies use gp130 family members (e.g., IL-
84 11, IL-6) in HSC maintenance conditions, including our own studies which typically use
85 20ng/mL of IL-11 alongside 300ng/mL of SCF (D. G. Kent *et al.*, 2008; Kent *et al.*, 2013;
86 Shepherd *et al.*, 2018). To test the absence of SCF and TPO, we cultured single mouse bone
87 marrow CD45⁺EPCR⁺CD48⁻CD150⁺Sca1^{high} long term HSCs (LT-HSCs), which are ~60%
88 functional HSCs by single cell transplantation (Wilson *et al.*, 2015), in the presence of 20
89 ng/mL IL-11 alone in both serum-containing (Kent *et al.*, 2013; Shepherd *et al.*, 2018) and
90 serum-free conditions (Wilkinson *et al.*, 2019) (Figure 1A). Between 20 and 40% of single LT-
91 HSCs survived 7 days of culture (Figure 1B), making them considerably more resilient to
92 cytokine depletion than single sorted progenitor cell fractions (Lin⁻Sca1⁺c-Kit⁺), where no cells
93 survived past 2 days (data not shown). Interestingly, 99.2% (634 of 639 cells) of the surviving
94 input LT-HSCs were maintained as single cells for the 7-day period (Figure 1C), and single-cell
95 time-lapse imaging and tracking confirmed that cells did not undergo division followed by
96 death of one daughter cell (Supplementary appendix 1). Together this prompted us to term
97 the minimal cytokine condition as a “hibernation” condition, similar to the cellular state of LT-
98 HSCs described after the addition of lipid raft inhibitors (Yamazaki *et al.*, 2006).

99 To assess the functional potential of single LT-HSCs in the hibernation condition (hibHSCs),
100 300ng/mL SCF was added to mirror cytokine combinations previously applied to freshly
101 isolated LT-HSCs (D. Kent *et al.*, 2008; Kent *et al.*, 2013; Shepherd *et al.*, 2018). Time to first
102 and second division was indistinguishable from freshly isolated LT-HSCs receiving SCF (Figure
103 1D) and clonal proliferation and survival over the subsequent 10 days was also similar, as
104 indicated by clone size distribution being nearly identical to freshly isolated HSCs stimulated
105 for 10 days (Figure 1E). In accordance with this, single hibHSCs also retained their multi-
106 potency in colony-forming cell (CFC) assays (Figure 1F-G) and 60-70% of single cells generated
107 at least three different lineages (Figure 1H) as determined by flow cytometry. Together, these
108 data suggest that HSCs surviving cytokine depletion exist in a state of prolonged hibernation
109 and can be revived to function indistinguishably from freshly isolated HSCs.

110

111 **Hibernating HSCs are fully functional in transplantation assays**

112 To assess whether cells cultured in the absence of SCF or TPO retained their HSC self-renewal
113 expansion capability, single day-7 hibHSCs were transplanted and their repopulation capacity
114 was compared to freshly isolated HSCs (Figure 2A). 62.5% (15/24) and 45.8% (13/29) of
115 primary recipients transplanted with single hibHSCs (without serum and with serum
116 respectively) had >1% multi-lineage donor chimerism at 16-24 weeks post-transplantation
117 compared to 48.8% (33/69) of freshly isolated HSCs (Figure 2B). Secondary transplantation
118 efficiency was also high (Figure 2C), suggesting that the period of 7 days *in vitro* had no impact
119 on HSC self-renewal. This was further supported by the observation of no significant
120 differences in mature cell production between hibHSCs and freshly isolated HSCs as
121 determined by the relative proportions of HSC subtype produced in single cell transplantation
122 experiments (Figure 2D). Notably, despite these high functional purities, the total yield of
123 functional HSCs was slightly lower considering that some HSCs do not survive hibernation.
124 These data provide formal evidence that following 7 days of SCF and TPO depletion and in the
125 complete absence of a supportive stem cell niche, LT-HSCs can retain full functional potential
126 as assessed by serial transplantation.

127

128 **High CD150 expression prospectively enriches for resilient HSCs**

129 Since only a proportion of phenotypic LT-HSCs survive hibernation conditions, we used flow
130 cytometric index sort data to determine whether levels of specific cell surface markers might
131 associate with survival. Expression levels of the SCF receptor (c-Kit) did not select for surviving
132 HSCs, while higher CD45 and EPCR expression were modestly increased on hibHSCs compared
133 to cells that did not survive hibernation conditions (data not shown). High CD150 expression
134 strongly associated with higher survival at day 7 (Figure 3A). To verify whether CD150 could
135 be used to prospectively enrich for resilient HSCs, single LT-HSCs were sorted as CD150^{mid} or
136 CD150^{high} and cultured in hibernation conditions. CD150^{high} HSCs show significantly higher
137 (4.2 fold) survival on day 7 compared to CD150^{mid} HSCs, confirming that CD150 expression can
138 enrich for phenotypic LT-HSCs that could survive hibernation conditions (Figure 3B). We next
139 assessed whether CD150 levels on surviving LT-HSCs associated with successful
140 transplantation and found no significant differences in CD150 intensity between HSCs that
141 successfully repopulated recipients versus those that did not (Figure 3C). Interestingly, when

142 we compared the cell division kinetics and 10 day colony size of single HSCs with high versus
143 low expression of CD150, we observed smaller colonies from cells expressing high levels of
144 CD150 (Figure 3D-E). Together these data suggest that while higher CD150 expression can
145 isolate cells enriched for resilient LT-HSCs with lower *in vitro* proliferation, the cells with lower
146 CD150 expression that survive do not have compromised transplantation ability, which is
147 supported by previous datasets examining CD150 expression in freshly isolated and
148 transplanted HSCs (Beerman *et al.*, 2010; Morita, Ema and Nakauchi, 2010; Wilson *et al.*,
149 2015).

150

151 **Hibernating LT-HSCs can be transduced without undergoing division**

152 To further explore the experimental and clinical potential of hibHSC culture conditions, we
153 next assessed whether transgenes could be delivered during the hibernation period. Small
154 bulk populations of LT-HSCs were isolated and exposed to a GFP-containing lentivirus for 2
155 days and then re-sorted into single cell cultures to determine single cell transduction
156 efficiencies and survival (Figure 4A). Following 10 days, 40% of the original sorted clones
157 (284/657) successfully produced colonies, with ~17.6% (50/284) of the surviving clones being
158 GFP⁺ (Figure 4B). In a second experiment to assess the *in vivo* functional potential of
159 transduced hibernating LT-HSCs, bulk cells were transplanted following the 2-day
160 transduction and assessed for GFP⁺ donor cell repopulation at 4, 8, and 16 weeks post-
161 transplantation (Figure 4A). All recipient mice were positive with initial reconstitution levels
162 ranging from 2 to 6% GFP⁺ cells (Figure 4C-D) and this contribution was stable throughout the
163 monitoring period, although early time points appear slightly higher suggesting that HSCs with
164 less durable self-renewal might be preferentially transduced. Together these data
165 demonstrate that lentiviral constructs can be successfully delivered to LT-HSCs in hibernation
166 cultures without cell division.

167

168 **Hibernating LT-HSCs share a core gene expression programme with freshly isolated LT-HSCs**

169 LT-HSCs deprived of SCF and TPO in hibernation conditions retain their functional properties,
170 including the ability to reconstitute primary and secondary recipients (Figure 2B-C). Aside
171 from IL-11, these LT-HSCs were cultured without signals from the hematopoietic niche or
172 neighbouring cells, making the transcriptome of these LT-HSCs a useful comparator for
173 determining which genes might be dispensable for LT-HSC function. To address this question,

174 we performed single-cell RNA-sequencing on LT-HSCs cultured in serum-free hibernating
175 conditions for 7 days (n=106) and compared them to freshly isolated single LT-HSCs (n=165)
176 and also to LT-HSCs stimulated with SCF for 16 hours (from both HSC+SCF (n=63) and
177 hibHSC+SCF(n=127) to determine the common pathways of activation upon SCF stimulation.
178 In order to determine broad differences between cell fractions, we performed dimensionality
179 reduction using Uniform Manifold Approximation and Projection (UMAP) on single cells from
180 all four conditions. Cells from each physiological setting clustered together in a unique space
181 (Figure 5A and Supplementary Figure 1A). These data indicate that while there is substantial
182 similarity to the molecular profile of freshly isolated HSCs, there are some molecular changes
183 that result from being removed from the *in vivo* microenvironment for 7 days.

184 To assess the similarity of hibHSCs to freshly isolated HSCs further, we compared the
185 expression levels of key HSC regulators that comprise the previously reported Molecular
186 Overlap (MoIO) gene signature (Wilson *et al.*, 2015). Overlaying MoIO scores on the UMAP
187 plot shows that the highest MoIO scores are present in the freshly isolated HSCs followed by
188 the hibHSCs and then their SCF-stimulated counterparts (Figure 5B). This pattern is mirrored
189 in the violin plots displaying individual single cell MoIO scores by physiological condition
190 (Figure 5C). Individual genes comprising the MoIO score and their relative expression across
191 the four biological states are provided in Supplementary Figure 1B. The relatively high MoIO
192 scores in hibHSCs indicates the utility of the MoIO score for identifying functional HSCs
193 irrespective of their physiological state. The similarity in these molecular features also
194 suggests that other factors must be contributing to the clear separation between freshly
195 isolated HSCs and hibHSCs.

196 Another example of molecular similarity between hibHSCs and freshly isolated HSCs was
197 evident when components of the cell cycle machinery were assessed to predict the cell cycle
198 stage of each profiled LT-HSC (Nestorowa *et al.*, 2016; Hamey and Göttgens, 2019). Again,
199 UMAP clustering (Figure 5D) shows that cell cycle status is not the primary driver of molecular
200 differences between freshly isolated and hibHSCs, with the vast majority of cells in both cases
201 being in the G₀/G₁ phase of the cell cycle (Supplementary Figure 1C). Overall, more than 80%
202 of freshly isolated HSCs and hibHSCs had molecular profiles consistent with being in the G₀/G₁
203 phase of the cell cycle (Figure 5E), whereas both SCF-stimulated HSC fractions had fewer than
204 40% G₀/G₁ cells. These data also accord with the cell cycle kinetics observed in Figure 1D
205 where cells that divide early in the curve (i.e., between 20 and 30 hours post stimulation)

206 would be expected to have progressed to the S or G₂ phase by 16 hours post-stimulation. This
207 is further emphasised by the heat map in Figure 5E which displays the HSC proliferation gene
208 signature from Venezia et al.(Venezia *et al.*, 2004) where both freshly isolated and hibHSCs
209 express low levels of proliferation-related genes (Figure 5F and Supplementary Figure 2A-E).
210 Finally, we also assessed markers of autophagy and senescence and in neither case did we
211 observe a significant enrichment (Supplementary Figure 3A-B)

212

213 **Hibernation cultures resolve common pathways of cytokine activation**

214 Historically, the molecular impact of adding specific cytokines to HSCs has been performed
215 following their direct isolation from the *in vivo* microenvironment. However, the impact that
216 membrane dynamics, protein turnover, and transcriptional priming would have on the
217 response of an HSC to a particular extracellular signal remains unclear. Hibernation cultures
218 offer a different physiological state of highly purified HSCs from which to understand the
219 direct impact of cytokine addition to a functional HSC. First, we observed the impact of
220 culturing HSCs in IL-11 alone during the hibernation condition, allowing us to resolve the
221 pathways activated or suppressed in response to IL-11 (Supplementary Figure 3C-E). Next,
222 using SCF as a stimulant, we profiled freshly isolated HSCs and hibHSCs to identify individual
223 gene expression patterns associated with SCF-stimulation (HSC+SCF, hibHSC+SCF). We first
224 generated differentially expressed gene lists from the HSC vs HSC+SCF and hibHSC vs.
225 hibHSC+SCF (Figure 6A). 27 genes were commonly differentially expressed (13 up and 14
226 down) upon addition of SCF with an expected activation of ATP generation and nucleotide
227 metabolism alongside a number of positive cell cycle mediators (*Mcm2*, *Mcm4*, *Mcm10*,
228 *Rad51*, *Rad51ap1*) and a reduction in developmental and MAPK-mediated signalling (Figure
229 6B and Supplementary Figure 4A). In addition to these expected changes, we also identified
230 SCF targets specifically induced in HSCs (Supplementary Figure 4A) and show that expression
231 of Mif (Ohta *et al.*, 2012) (an inflammatory cytokine promoting survival and proliferation) and
232 Txn1 (Schenk *et al.*, 1994) (regulator of AP-1 signalling) are directly promoted upon SCF
233 addition to functional HSCs.

234

235 **Hibernating HSCs downregulate AP1 complex and other stem cell regulators**

236 Despite the strong overlap in cell cycle and MoIO gene signature expression, hibHSCs form a
237 distinct cluster away from freshly isolated HSCs (Figure 5A and Supplementary Figure 4B).

238 While some of this distance could be attributable to downregulation of specific MoLO genes
239 (including *Sult1a1* and *Gimap1*, Figure 6D), global differential gene expression analysis
240 between HSCs and hibHSCs identified 116 upregulated and 138 downregulated genes (Figure
241 6C). Amongst those additional genes whose expression was significantly reduced, a number
242 of AP-1 complex members were identified, including *Jun* and *Fos* and their co-regulator *Ncor2*
243 as well as molecules with previously described roles in HSC biology such as *Cish* (Scheppers *et*
244 *al.*, 2012) and *Vwf* (Figure 6D and Supplementary Figure 4C). Since hibHSCs retain their
245 functional properties *in vivo*, these data suggest that high levels of these genes are not a
246 requirement for HSC function. On the other hand, pathways that were highly upregulated in
247 hibHSCs were associated with stress response and nutrient deprivation, consistent with being
248 kept in minimal cytokine conditions and KEGG pathway analysis identified cAMP and mTOR
249 signalling (Dhawan and Laxman, 2015) alongside Glycolysis and Fatty Acid Biosynthesis (Figure
250 6E). This accords with enrichment of HSC pro-survival genes *ler3* and *Pdcd1lg2* expression in
251 hibernating HSCs. Of additional interest, multiple HLF target genes, including *Lyz1* and *Lrrc8a*,
252 were overexpressed in hibernated HSCs, potentially supporting the notion that HSCs are
253 exerting a stress response to maintain survival/quiescence (Komorowska *et al.*, 2017) in
254 response to cytokine deprivation (Figure 6F and Supplementary Figure 5).

255

256 **Human HSCs can be retained as single cells in hibernation conditions**

257 To investigate whether cytokine deprivation had a similar effect on human HSCs, we isolated
258 single human CD34⁺CD38⁻CD90⁺CD45RA⁻CD19⁻CD49f⁺ cells (hHSCs) from cord blood and
259 cultured them in serum-free medium with human IL-11 alone for 7 days (Figure 7A). Similar
260 to mouse LT-HSCs, survival was lower with cytokine deprivation (Figure 7B) and, although
261 some cells divided (~25.6%, Figure 7C), a large proportion remained as single cells compared
262 to hHSCs under standard cytokine conditions (Ortmann *et al.*, 2015; Belluschi *et al.*, 2018).
263 The fact that some hHSCs divided may be due to the starting purity or activation state of HSCs
264 from cord blood. Upon transplantation of limited numbers of day 7 cultured human HSCs,
265 repopulation was stable out to 20 weeks post-transplantation, but donor repopulation was
266 below detection for the lowest dose recipients (Figure 7D). Together these results
267 demonstrate that IL-11 alone can maintain a proportion of multi-potent human HSCs in a non-
268 dividing state, but further culture optimisation would be required to support retention of
269 large numbers of fully functional human HSCs.

270 **Discussion**

271 Recent studies have produced a substantial amount of single cell gene expression data from
272 normal and malignant hematopoietic cells isolated from the mouse bone marrow (Shepherd
273 and Kent, 2019). As a result, the transcriptional program of a quiescent “steady-state” LT-HSC
274 is firmly established. Which genes drive individual LT-HSC properties (e.g., quiescence, self-
275 renewal, differentiation, stress response, etc) is much less well understood, and is
276 complicated by only being able to obtain highly purified functional LT-HSCs from a single
277 physiological state (i.e., quiescent cells from the BM niche). Indeed, studies that have
278 compared LT-HSCs to their downstream progenitors have identified “cell cycle” changes as
279 the dominant molecular feature separating LT-HSCs from non-HSCs (Passegué *et al.*, 2005;
280 Wilson *et al.*, 2015). Hibernation cultures allow us to isolate and maintain functional LT-HSCs
281 for prolonged periods of time in the absence of other cells without undergoing cell division or
282 differentiation, thereby allowing the resolution of the common molecular programme of HSCs
283 in different physiological state. We identify molecules potentially dispensable for HSC
284 function and a common molecular programme of SCF activation in purified HSCs from distinct
285 states. Finally, our study also resolves a debate about the impact of serum exposure on the
286 cell fate of LT-HSCs (Domen and Weissman, 2000; Rogers, Yamanaka and Casper, 2008; Ieyasu
287 *et al.*, 2017), showing that LT-HSCs can be cultured in the presence of serum for 7 days without
288 undergoing differentiation or proliferation.

289 Distinct endogenous signalling pathways have been shown to regulate LT-HSC survival,
290 self-renewal, and proliferation in both mouse (Wohrer *et al.*, 2014) and human (Knapp *et al.*,
291 2017). A similar cellular phenomenon of hibernation was observed when LT-HSCs were
292 exposed to inhibitors that blocked lipid raft clustering (even in the presence of SCF) and
293 remained undifferentiated as single cells for 5-7 days in culture (Yamazaki *et al.*, 2006).
294 Despite being deprived completely of TPO and SCF signalling, our hibernation cultures contain
295 IL-11, without which all cells die within 48 hours. One of the key pathways activated by IL-11
296 is gp130, which has been historically implicated in a wide array of stem cell systems, including
297 mouse ES cells with LIF (Nichols *et al.*, 2001), the Drosophila germ stem cell niche with Upd
298 (Amoyel and Bach, 2012), mouse neural stem cells with CTNF and LIF (Shimazaki, Shingo and
299 Weiss, 2001), mouse muscle stem cells with OSM (Sampath *et al.*, 2018) and mouse HSCs with
300 IL-6 and IL-11 (Yoshida *et al.*, 1996; Audet *et al.*, 2001). Of particular interest, OSM was shown

301 to promote muscle cell engraftment without inducing proliferation (Sampath *et al.*, 2018),
302 lending additional support to the hypothesis that gp130 stimulants may regulate survival of
303 quiescent stem cells in multiple stem cell systems.

304 Whereas other *in vitro* conditions have been shown to maintain mouse LT-HSCs, these
305 systems uniformly create populations of cells in which LT-HSCs are the vast minority of the
306 final culture (Gundry *et al.*, 2016; Bak, Dever and Porteus, 2018; Wagenblast *et al.*, 2019;
307 Wilkinson *et al.*, 2019). In the absence of a robust *in vitro* LT-HSC purification strategy,
308 molecular studies are therefore compromised by large numbers of contaminating non-HSCs.
309 Our study averts this issue by retaining functional LT-HSCs as single cells. The gene expression
310 programs of single functional LT-HSCs in 7-day hibernation conditions show a high retention
311 of known self-renewal regulators, and are consistent with the cells being in G₀/G₁. They also
312 identify several regulators whose absence does not impact HSC engraftment or serially
313 repopulation. One such set of factors was the AP1 complex, where expression of several
314 members including *Jun*, *Fos*, and *Ncor2* was significantly reduced in hibernation cultures. This
315 is potentially due to the hibernation cultures driving their extinguished expression and cells
316 that do not have sufficient amounts of AP1 complex members do not survive. In contrast, *in*
317 *vivo* loss or reduced AP1 function leads to increased proliferation and differentiation
318 (Santaguida *et al.*, 2009). It may be that expression of these molecules is rescued upon
319 transplantation when HSCs expand, although the SCF-induced entry into cell cycle does not
320 on its own initiate their expression.

321 A previous studies has reported that low cytokine concentration in culture facilitates
322 the maintenance of engraftable mouse and human HSCs (Kobayashi *et al.*, 2019) with reduced
323 proliferation *in vitro* and this finding is supported by studies showing that slow-dividing LT-
324 HSC clones were much more likely to retain HSC function (Dykstra *et al.*, 2006; Laurenti *et al.*,
325 2015). However, none of these studies were able to retain single LT-HSCs at high purities with
326 indistinguishable properties from freshly isolated LT-HSCs, making it impossible to perform
327 molecular studies on single functional HSCs or to manipulate them at the single cell level.
328 Hibernation cultures permit such analyses since single LT-HSCs do not lose any functional
329 capacity with a highly similar, if not slightly improved, primary and secondary transplantation
330 capacity compared to freshly isolated HSCs.

331 The finding that high CD150 expression levels prospectively identify resilient HSCs that
332 survive hibernation are broadly consistent with data that implicates CD150 as a marker of LT-

333 HSCs with more durable self-renewal capacity in serial transplantation assays (Kent *et al.*,
334 2009; Beerman *et al.*, 2010; Morita, Ema and Nakauchi, 2010). The highest levels of CD150
335 also associated with a delayed engraftment in primary transplantations, an initial deficiency
336 in making lymphoid cells (Kent *et al.*, 2009; Morita, Ema and Nakauchi, 2010), and an ability
337 to create daughter HSCs with full multi-lineage potential (Dykstra *et al.*, 2007; Komorowska
338 *et al.*, 2017). This further accords with the increased number of α -HSCs (myeloid-biased)
339 observed in our transplantation data. The delay in engraftment observed generally in α -HSCs
340 may be related to the dynamics of quiescence/activation of daughter LT-HSCs in a
341 transplantation scenario and our *in vitro* hibernation system offers the chance to study HSC
342 activation in a distinct physiological context with unprecedented resolution. This latter
343 capacity is particularly important in the context of HSC transplantation where cells need to
344 exit, and eventually return to, quiescence during any sort of *in vitro* culture period and
345 subsequent re-seeding of recipient bone marrow.

346 Optimisation of hibernation cultures for manipulating highly purified LT-HSCs would
347 also have a wide range of applications in experimental and clinical research. The knowledge
348 that LT-HSCs are fully functional during hibernation offers the opportunity to manipulate
349 them at the single cell level with precise assessment of the impact of specific modifications.
350 Our data show that genetic modification can be undertaken in hibernation cultures which
351 could potentially set the stage for the delivery of multiple viral constructs during the culture
352 period. This would permit studies of combinatorial genetic modifications in highly purified LT-
353 HSCs, as opposed to a heterogeneous pool of stem and progenitor cells typically assayed in
354 such protocols. Finally, we provide proof-of-principle evidence that hibernation cultures can
355 be adapted to the human setting, offering substantial potential for implementing genetic
356 modifications in human HSCs and setting the stage for more precise interrogation of the
357 functional properties of individual LT-HSCs.

358

359 **Experimental Procedures**

360 **Mice**

361 C57BL/6-Ly5.2 (WT) were purchased from Charles River (Saffron Walden, Essex, UK).
362 C57BL/6w41/w41-Ly5.1 (W41) were bred and maintained at the University of Cambridge. Full
363 details are available in the Supplementary Data.

364

365 **Isolation of mouse Sca1^{high} ESLAM HSCs, *in vitro* assays, and expression profiling**

366 HSCs were isolated from the lineage depleted cell suspension by using fluorescence-activated
367 cell sorting (FACS) using EPCR^{high}, CD45⁺, Sca-1^{high}, CD48^{low/neg}, CD150⁺ (or “ESLAM”), as
368 described previously (Kent *et al.*, 2009) with full details found in the Supplementary Data.

369

370 **Bone marrow transplantation assays and analysis**

371 Donor cells were obtained from C56BL/6J mice (CD45.2). Recipient mice were
372 C57Bl6W41/W41 (W41) mice as described previously (Kent *et al.*, 2009; Benz *et al.*, 2012).
373 Full details of transplantation and peripheral blood analysis are in the Supplementary Data.

374

375 **Lentiviral transduction of mouse HSCs**

376 ESLAM HSCs (7000 cells) were isolated and transduced with GFP-containing lentivirus; full
377 details of transduction method and assays are in the Supplementary Data.

378

379 **Isolation of human CB HSCs and *in vitro* assays**

380 Cord blood samples were obtained from Cambridge Blood and Stem Cell Biobank (CBSB) with
381 informed consent from healthy donors in accordance with regulated procedures approved by
382 the relevant Research and Ethics Committees. Details of HSC isolation and *in vitro* assays are
383 found in the Supplementary Data.

384

385 **Single cell RNA-sequencing**

386 Single cell RNA sequencing analysis was performed as described previously in Picelli *et al.*
387 2014 (Smart-seq2), with full details in the Supplementary Data. Data are publicly available
388 using the GEO accession number: GSE160131.

389

390 **Xenotransplantation and analysis**

391 Donor cells were obtained from CD34-enriched CB samples. Recipient mice were NSG. Full
392 details of transplantation and peripheral blood analysis are found in the Supplementary Data.

393

394 **Acknowledgments**

395 We thank Reiner Schulte, Chiara Cossetti, and Gabriela Grondys-Kotarba of the CIMR Flow
396 Cytometry core and Anna Petrunkina-Harrison in the NIHR BRC Cell Phenotyping Hub for
397 technical assistance and suggestions; Tina Hamilton, Dean Pask, Nicole Mende, Emily
398 Calderbank, Carys Johnson, Rebecca Hannah and Winnie Lau for technical assistance; Sally
399 Thomas and the Central Biomedical Services unit staff; Joanna Baxter and the Cambridge
400 Blood and Stem Cell Biobank staff; and Nicola Wilson, Fernando Calero-Nieto, Robert
401 Oostendorp, and Emmanuelle Passegué for helpful discussion. C.A.O. and D.B. were
402 supported by Wellcome PhD Studentships, F.K.H. was supported by a Medical Research
403 Council (MRC) PhD Studentship, M.S.S. was the recipient of a Biotechnology and Biological
404 Sciences Research Council Industrial Collaborative Awards in Science and Engineering PhD
405 Studentship, S.B. was supported by a CRUK Cambridge Cancer Centre PhD Studentship and
406 J.L.C.C. was supported by an MRC PhD Studentship under the University of Cambridge
407 Doctoral Training Programme. Research in the B.G. lab is supported by Wellcome, Blood
408 Cancer UK, and an MRC-AMED joint award (MR/V005502/1). E.L. is supported by a
409 Wellcome / Royal Society Sir Henry Dale Fellowship (107630/Z/15/Z) and work in her
410 laboratory is also supported by the European Hematology Association and BBSRC
411 (BB/P002293/1). The D.G.K. laboratory is supported by a Blood Cancer UK Bennett
412 Fellowship (15008), an ERC Starting Grant (ERC-2016-STG-715371), and an MRC-AMED joint
413 award (MR/V005502/1). D.G.K. E.L., and B.G. are supported by a core support grant to the
414 Wellcome MRC Cambridge Stem Cell Institute, Blood Cancer UK, the NIHR Cambridge
415 Biomedical Research Centre, and the CRUK Cambridge Cancer Centre.

416

417 **Author contributions**

418 Contribution: C.A.O, M.B., D.G.K., and E.L. conceived and designed the experiments; C.A.O.,
419 M.B., M.S.S., J.L.C.C., G.B., C.M., and S.B. performed the experiments; C.A.O., M.B., D.B.,
420 F.K.H., E.D., and H.P.B., analysed the data; M.B., D.B., and D.G.K. wrote the paper with input
421 from E.L. and B.G.

422

423 **Declaration of Interests**

424 The authors declare no competing interests.

425

426 **References**

- 427 Amoyel, M. and Bach, E. (2012) 'Functions of the Drosophila JAK-STAT pathway: Lessons from
428 stem cells', *JAK-STAT*. doi: 10.4161/jkst.21621.
- 429 Audet, J. *et al.* (2001) 'Distinct role of gp130 activation in promoting self-renewal divisions by
430 mitogenically stimulated murine hematopoietic stem cells', *Proceedings of the National
431 Academy of Sciences of the United States of America*, 98(4), pp. 1757–1762. doi:
432 10.1073/pnas.98.4.1757.
- 433 Bak, R. O., Dever, D. P. and Porteus, M. H. (2018) 'CRISPR/Cas9 genome editing in human
434 hematopoietic stem cells', *Nature Protocols*. doi: 10.1038/nprot.2017.143.
- 435 Beerman, I. *et al.* (2010) 'Functionally distinct hematopoietic stem cells modulate
436 hematopoietic lineage potential during aging by a mechanism of clonal expansion',
437 *Proceedings of the National Academy of Sciences of the United States of America*, 107(12), pp.
438 5465–5470. doi: 10.1073/pnas.1000834107.
- 439 Belluschi, S. *et al.* (2018) 'Myelo-lymphoid lineage restriction occurs in the human
440 haematopoietic stem cell compartment before lymphoid-primed multipotent progenitors',
441 *Nature Communications*, 9(1), pp. 1–15. doi: 10.1038/s41467-018-06442-4.
- 442 Benz, C. *et al.* (2012) 'Hematopoietic stem cell subtypes expand differentially during
443 development and display distinct lymphopoietic programs', *Cell Stem Cell*, 10(3), pp. 273–283.
444 doi: 10.1016/j.stem.2012.02.007.
- 445 Butler, A. *et al.* (2018) 'Integrating single-cell transcriptomic data across different conditions,
446 technologies, and species', *Nature Biotechnology*, 36(5), pp. 411–420. doi: 10.1038/nbt.4096.
- 447 Cheung, T. H. and Rando, T. A. (2013) 'Molecular regulation of stem cell quiescence', *Nature
448 Reviews Molecular Cell Biology*, 14(6), pp. 329–340. doi: 10.1038/nrm3591.
- 449 Dhawan, J. and Laxman, S. (2015) 'Decoding the stem cell quiescence cycle - Lessons from
450 yeast for regenerative biology', *Journal of Cell Science*, 128(24), pp. 4467–4474. doi:
451 10.1242/jcs.177758.
- 452 Domen, J. and Weissman, I. L. (2000) 'Hematopoietic stem cells need two signals to prevent
453 apoptosis; BCL-2 can provide one of these, Kitl/c-Kit signaling the other', *Journal of
454 Experimental Medicine*. doi: 10.1084/jem.192.12.1707.
- 455 Doulatov, S. *et al.* (2012) 'Hematopoiesis: A human perspective', *Cell Stem Cell*. *Cell Stem Cell*,
456 pp. 120–136. doi: 10.1016/j.stem.2012.01.006.

457 Dykstra, B. *et al.* (2006) 'High-resolution video monitoring of hematopoietic stem cells
458 cultured in single-cell arrays identifies new features of self-renewal', *Proceedings of the*
459 *National Academy of Sciences of the United States of America*. doi:
460 10.1073/pnas.0602548103.

461 Dykstra, B. *et al.* (2007) 'Long-Term Propagation of Distinct Hematopoietic Differentiation
462 Programs In Vivo', *Cell Stem Cell*, 1(2), pp. 218–229. doi: 10.1016/j.stem.2007.05.015.

463 Eaves, C. J. (2015) 'Hematopoietic stem cells: Concepts, definitions, and the new reality',
464 *Blood*, 125(17), pp. 2605–2613. doi: 10.1182/blood-2014-12-570200.

465 Fares, I. *et al.* (2017) 'EPCR expression marks UM171-expanded CD34+ cord blood stem cells',
466 *Blood*, 129(25), pp. 3344–3351. doi: 10.1182/blood-2016-11-750729.

467 Ganuza, M. *et al.* (2020) 'Clones assemble! The clonal complexity of blood during ontogeny
468 and disease', *Experimental Hematology*, 83, pp. 35–47. doi: 10.1016/j.exphem.2020.01.009.

469 De Graaf, C. A. and Metcalf, D. (2011) 'Thrombopoietin and hematopoietic stem cells', *Cell*
470 *Cycle*. Taylor and Francis Inc., pp. 1582–1589. doi: 10.4161/cc.10.10.15619.

471 Gundry, M. C. *et al.* (2016) 'Highly Efficient Genome Editing of Murine and Human
472 Hematopoietic Progenitor Cells by CRISPR/Cas9', *Cell Reports*. doi:
473 10.1016/j.celrep.2016.09.092.

474 Hamey, F. K. and Göttgens, B. (2019) 'Machine learning predicts putative hematopoietic stem
475 cells within large single-cell transcriptomics data sets', *Experimental Hematology*, 78, pp. 11–
476 20. doi: 10.1016/j.exphem.2019.08.009.

477 Ieyasu, A. *et al.* (2017) 'An All-Recombinant Protein-Based Culture System Specifically
478 Identifies Hematopoietic Stem Cell Maintenance Factors', *Stem Cell Reports*. doi:
479 10.1016/j.stemcr.2017.01.015.

480 Kent, D. *et al.* (2008) 'Regulation of hematopoietic stem cells by the steel factor/KIT signaling
481 pathway', *Clinical Cancer Research*. Clin Cancer Res, pp. 1926–1930. doi: 10.1158/1078-
482 0432.CCR-07-5134.

483 Kent, D. G. *et al.* (2008) 'Steel factor coordinately regulates the molecular signature and
484 biologic function of hematopoietic stem cells', *Blood*, 112(3), pp. 560–567. doi:
485 10.1182/blood-2007-10-117820.

486 Kent, D. G. *et al.* (2009) 'Prospective isolation and molecular characterization of
487 hematopoietic stem cells with durable self-renewal potential', *Blood*, 113(25), pp. 6342–
488 6350. doi: 10.1182/blood-2008-12-192054.

489 Kent, D. G. *et al.* (2013) 'Self-Renewal of Single Mouse Hematopoietic Stem Cells Is Reduced
490 by JAK2V617F Without Compromising Progenitor Cell Expansion', *PLoS Biology*. Edited by M.
491 A. Goodell, 11(6), p. e1001576. doi: 10.1371/journal.pbio.1001576.

492 Knapp, D. J. H. F. *et al.* (2017) 'Dissociation of Survival, Proliferation, and State Control in
493 Human Hematopoietic Stem Cells', *Stem Cell Reports*. doi: 10.1016/j.stemcr.2016.12.003.

494 Kobayashi, H. *et al.* (2019) 'Environmental Optimization Enables Maintenance of Quiescent
495 Hematopoietic Stem Cells Ex Vivo', *Cell Reports*, 28(1), pp. 145-158.e9. doi:
496 10.1016/j.celrep.2019.06.008.

497 Komorowska, K. *et al.* (2017) 'Hepatic Leukemia Factor Maintains Quiescence of
498 Hematopoietic Stem Cells and Protects the Stem Cell Pool during Regeneration', *Cell Reports*,
499 21(12), pp. 3514–3523. doi: 10.1016/j.celrep.2017.11.084.

500 Laurenti, E. *et al.* (2015) 'CDK6 levels regulate quiescence exit in human hematopoietic stem
501 cells', *Cell Stem Cell*. doi: 10.1016/j.stem.2015.01.017.

502 Laurenti, E. and Göttgens, B. (2018) 'From haematopoietic stem cells to complex
503 differentiation landscapes', *Nature*. Nature Publishing Group, pp. 418–426. doi:
504 10.1038/nature25022.

505 Love, M. I., Huber, W. and Anders, S. (2014) 'Moderated estimation of fold change and
506 dispersion for RNA-seq data with DESeq2', *Genome Biology*, 15(12), p. 550. doi:
507 10.1186/s13059-014-0550-8.

508 Mootha, V. K. *et al.* (2003) 'PGC-1 α -responsive genes involved in oxidative phosphorylation
509 are coordinately downregulated in human diabetes', *Nature Genetics*, 34(3), pp. 267–273.
510 doi: 10.1038/ng1180.

511 Morita, Y., Ema, H. and Nakauchi, H. (2010) 'Heterogeneity and hierarchy within the most
512 primitive hematopoietic stem cell compartment', *Journal of Experimental Medicine*, 207(6),
513 pp. 1173–1182. doi: 10.1084/jem.20091318.

514 Nestorowa, S. *et al.* (2016) 'A single-cell resolution map of mouse hematopoietic stem and
515 progenitor cell differentiation', *Blood*, 128(8), pp. e20–e31. doi: 10.1182/blood-2016-05-
516 716480.

517 Nichols, J. *et al.* (2001) 'Physiological rationale for responsiveness of mouse embryonic stem
518 cells to gp130 cytokines', *Development*.

519 Ohta, S. *et al.* (2012) 'Macrophage migration inhibitory factor (MIF) promotes cell survival and
520 proliferation of neural stem/progenitor cells', *Development (Cambridge)*, 139(19). doi:

521 10.1242/jcs.102210.

522 Ortmann, C. A. *et al.* (2015) 'Effect of Mutation Order on Myeloproliferative Neoplasms', *New*
523 *England Journal of Medicine*, 372(7), pp. 601–612. doi: 10.1056/NEJMoa1412098.

524 Passegué, E. *et al.* (2005) 'Global analysis of proliferation and cell cycle gene expression in the
525 regulation of hematopoietic stem and progenitor cell fates', *Journal of Experimental*
526 *Medicine*, 202(11), pp. 1599–1611. doi: 10.1084/jem.20050967.

527 Rogers, I. M., Yamanaka, N. and Casper, R. F. (2008) 'A Simplified Procedure for Hematopoietic
528 Stem Cell Amplification Using a Serum-Free, Feeder Cell-Free Culture System', *Biology of*
529 *Blood and Marrow Transplantation*. doi: 10.1016/j.bbmt.2008.06.002.

530 Sampath, Srinath C. *et al.* (2018) 'Induction of muscle stem cell quiescence by the secreted
531 niche factor Oncostatin M', *Nature Communications*. doi: 10.1038/s41467-018-03876-8.

532 Santaguida, M. *et al.* (2009) 'JunB Protects against Myeloid Malignancies by Limiting
533 Hematopoietic Stem Cell Proliferation and Differentiation without Affecting Self-Renewal',
534 *Cancer Cell*, 15(4), pp. 341–352. doi: 10.1016/j.ccr.2009.02.016.

535 Schenk, H. *et al.* (1994) 'Distinct effects of thioredoxin and antioxidants on the activation of
536 transcription factors NF- κ B and AP-1', *Proceedings of the National Academy of Sciences of the*
537 *United States of America*, 91(5), pp. 1672–1676. doi: 10.1073/pnas.91.5.1672.

538 Schepers, H. *et al.* (2012) 'STAT5-mediated self-renewal of normal hematopoietic and
539 leukemic stem cells', *JAK-STAT*, 1(1), pp. 13–25. doi: 10.4161/jkst.19316.

540 Shepherd, M. S. *et al.* (2018) 'Single-cell approaches identify the molecular network driving
541 malignant hematopoietic stem cell self-renewal', *Blood*, 132(8). doi: 10.1182/blood-2017-12-
542 821066.

543 Shepherd, M. S. and Kent, D. G. (2019) 'Emerging single-cell tools are primed to reveal
544 functional and molecular heterogeneity in malignant hematopoietic stem cells', *Current*
545 *Opinion in Hematology*, 26(4), pp. 214–221. doi: 10.1097/MOH.0000000000000512.

546 Shimazaki, T., Shingo, T. and Weiss, S. (2001) 'The ciliary neurotrophic factor/leukemia
547 inhibitory factor/gp130 receptor complex operates in the maintenance of mammalian
548 forebrain neural stem cells', *Journal of Neuroscience*. doi: 10.1523/jneurosci.21-19-
549 07642.2001.

550 Stuart, T. *et al.* (2019) 'Comprehensive Integration of Single-Cell Data', *Cell*, 177(7), pp. 1888-
551 1902.e21. doi: 10.1016/j.cell.2019.05.031.

552 Subramanian, A. *et al.* (2005) 'Gene set enrichment analysis: A knowledge-based approach

553 for interpreting genome-wide expression profiles', *Proceedings of the National Academy of*
554 *Sciences of the United States of America*, 102(43), pp. 15545–15550. doi:
555 10.1073/pnas.0506580102.

556 Tirosh, I. *et al.* (2016) 'Dissecting the multicellular ecosystem of metastatic melanoma by
557 single-cell RNA-seq', *Science*, 352(6282), pp. 189–196. doi: 10.1126/science.aad0501.

558 Venezia, T. A. *et al.* (2004) 'Molecular Signatures of Proliferation and Quiescence in
559 Hematopoietic Stem Cells', *PLoS Biology*. Edited by Bing Lim, 2(10), p. e301. doi:
560 10.1371/journal.pbio.0020301.

561 Wagenblast, E. *et al.* (2019) 'Functional profiling of single CRISPR/Cas9-edited human long-
562 term hematopoietic stem cells', *Nature Communications*. doi: 10.1038/s41467-019-12726-0.

563 Wilkinson, A. C. *et al.* (2019) 'Long-term ex vivo haematopoietic-stem-cell expansion allows
564 nonconditioned transplantation', *Nature*, 571(7763), pp. 117–121. doi: 10.1038/s41586-019-
565 1244-x.

566 Wilson, N. K. *et al.* (2015) 'Combined Single-Cell Functional and Gene Expression Analysis
567 Resolves Heterogeneity within Stem Cell Populations', *Cell Stem Cell*, 16(6), pp. 712–724. doi:
568 10.1016/j.stem.2015.04.004.

569 Wohrer, S. *et al.* (2014) 'Distinct Stromal Cell Factor Combinations Can Separately Control
570 Hematopoietic Stem Cell Survival, Proliferation, and Self-Renewal', *Cell Reports*, 7(6), pp.
571 1956–1967. doi: 10.1016/j.celrep.2014.05.014.

572 Yamazaki, S. *et al.* (2006) 'Cytokine signals modulated via lipid rafts mimic niche signals and
573 induce hibernation in hematopoietic stem cells', *EMBO Journal*, 25(15), pp. 3515–3523. doi:
574 10.1038/sj.emboj.7601236.

575 Yamazaki, S. *et al.* (2009) 'TGF- 2 as a candidate bone marrow niche signal to induce
576 hematopoietic stem cell hibernation', *Blood*, 113(6), pp. 1250–1256. doi: 10.1182/blood-
577 2008-04-146480.

578 Yoshida, K. *et al.* (1996) 'Targeted disruption of gp130, a common signal transducer for the
579 interleukin 6 family of cytokines, leads to myocardial and hematological disorders',
580 *Proceedings of the National Academy of Sciences of the United States of America*, 93(1), pp.
581 407–411. doi: 10.1073/pnas.93.1.407.

582

583 **Figure Titles and Legends**

584 **Figure 1: Absence of SCF and TPO maintains HSCs as single multi-potent cells *in vitro***

585 (A) Single CD45⁺EPCR⁺CD48⁻CD150⁺Sca1^{high} LT-HSCs were sorted into individual wells and

586 cultured in the presence of IL-11, in serum-supplemented or serum-free medium and in the

587 presence or absence of SCF. For SCF-supplemented cultures (green plate), daily cell counts

588 were performed for 10 days. For cultures only containing IL-11 (red plate), HSCs were supplied

589 with SCF on day 7 post-isolation after which daily cell counts were performed for an additional

590 10 days. In all cases, clone size was assessed at day 10 post-SCF addition. (B) HSC survival is

591 decreased in the absence of SCF compared to SCF-supplemented medium (+serum/+SCF

592 n=355, 5 biological replicates; +serum/-SCF n=1722, 7 independent experiments; -

593 serum/+SCF, N=144, 2 independent experiments, -serum/-SCF n=284, 3 independent

594 experiments). (C) Numbers of wells with >2 cells were scored to determine the number of

595 clones that had divided. At day 7 post-isolation, only culture conditions without SCF

596 maintained HSCs as single cells. (D) Cell division kinetics post-SCF addition. Entry into cell cycle

597 was comparable between freshly isolated HSCs (green solid line) and cells that had been

598 maintained as single cells for 7 days (orange solid line) in serum-supplemented media. Time

599 to subsequent cell division (dotted lines) was not significantly different between conditions

600 (SCF added at day 0, n=355, 5 independent experiments; SCF added at day 7, n=1722, 7

601 independent experiments). (E) Colony size was measured on day 10 post-SCF addition and no

602 difference in clone size distribution was observed between HSCs cultured in presence of SCF

603 from day 0 and post-hibernation HSCs (day 7 + 10). (F) Single LT-HSCs were cultured for 7 days

604 in IL-11 alone, in serum-supplemented or serum-free medium. After 7 days, single hibernating

605 LT-HSCs were individually transferred into a cytokine rich methyl-cellulose CFC assay and

606 cultured for an additional 14 days. On day 14, lineage composition of individual colonies was

607 assessed by flow cytometry. (G) Colony forming efficiency for freshly isolated single LT-HSCs,

608 single LT-HSCs cultured in serum-supplemented and serum-free hibernating cultures. (fresh,

609 n=300, 3 biological replicates; serum-free, n=121, 5 independent experiments; +serum,

610 n=230, 6 independent experiments). (H) Colony subtype analysis showed that the majority of

611 single cells (~80%) generated colonies of at least three lineages in CFU assays (hibHSC serum-

612 free, n=70, 4 independent experiments; hibHSC+serum, n=166, 3 independent experiments).

613 Colonies were defined as MK (containing cells positive for megakaryocyte marker CD41), GM

614 (containing cells positive for granulocyte/monocyte markers Gr1 and CD11b), GEM (positive

615 for GM and erythrocyte markers Gr1, CD11b, and Ter-119), GMM (positive for GM and MK

616 markers), and GEMM (positive for GM, MK, and E markers), as described in the methods. Bars
617 show mean with SEM. Unpaired t-test: * $p < 0.05$, ** $p < 0.01$, *** $p < 0.001$.

618

619 **Figure 2: Hibernating HSCs maintain *in vivo* functional activity**

620 (A) HSCs were cultured in hibernation conditions in either serum-supplemented or serum-
621 free medium. Single fresh or day 7 hibernating LT-HSCs were transplanted into W41-CD45.1
622 recipients (fresh $n=69$, serum-free $n=24$, +serum $n=29$). Secondary transplantations were
623 undertaken in all mice with donor engraftment ($>1\%$) at 16-24 weeks post-transplantation.
624 (B) and (C) Graphs show % donor chimerism in the peripheral blood of primary and secondary
625 recipient mice at 16-24 weeks post-transplantation. Recipients with chimerism $>1\%$ and at
626 least 0.5% of GM, B, and T cells were considered to be repopulated. (Triangles represent mice
627 where chimerism reached $>1\%$ at weeks 20-24 post-transplantation but had not done so by
628 16 weeks). (D) No significant difference was observed in the balance of mature cell outputs
629 between freshly isolated and post-hibernation HSCs. Based on donor myeloid (M) to lymphoid
630 (L) ratio at 16 weeks in primary recipients, the founder HSC was retrospectively assigned one
631 of the following subtypes: α (alpha, $M:L > 2$), β (beta, $M:L > 0.25 < 2$), γ (gamma, $M:L < 0.25$), δ
632 (delta, $M:L < 0.25$ and failure to contribute to myeloid lineage past 16 weeks) in accordance
633 with Dykstra et al., 2007 (Dykstra *et al.*, 2007) (HSC $n=31/69$; hibHSC(+serum) $n=12/29$;
634 hibHSC (serum-free) $n=15/24$).

635

636 **Figure 3: Higher expression of CD150 identifies resilient LT-HSCs**

637 (A) Flow cytometric index-sort data was used to determine the CD150 expression level of LT-
638 HSCs at the time of isolation. Cells which did not survive at Day 1 and Day 7 were compared
639 to those that survived out to Day 7 with the latter population of cells correlating with higher
640 CD150 expression. A boxplot shows the median with interquartile range (IQR). Vertical lines
641 represent outermost quartiles. Black dots, if present, are extreme outliers. Unpaired t-test:
642 * $p < 0.05$, ** $p < 0.01$, *** $p < 0.001$. (B) Prospectively sorted CD150^{high} LT-HSCs show 4.2-fold
643 higher survival than CD150^{mid} LT-HSCs ($n=480$, 5 independent experiments). Paired two-tailed
644 t-test. (C) Hibernating HSCs in serum-free and serum-supplemented conditions were
645 transplanted, and their CD150 levels retrospectively assessed. Cells able to repopulate a
646 recipient (black) did not differ in initial CD150 expression levels compared to cells unable to
647 repopulate (grey). (D) HSCs with high or low expression of CD150 were determined using

648 index-sorting data from freshly isolated HSCs that were cultured for 7 days in serum-free
649 medium supplemented with 20ng/mL IL-11 and 300 ng/mL SCF. Three biological replicates
650 were analysed, and in each case the top third and bottom third of CD150 expressers were
651 analysed as CD150^{high} and CD150^{low} respectively. Daily cell counts were performed to assess
652 cell division kinetics. Entry into cell cycle and the second division were not significantly altered
653 between CD150^{high} and CD150^{low} LT-HSCs. (E) Using the same experimental data from Figure
654 3D, colony sizes from single LT-HSCs were measured on day 10 and clone sizes from single LT-
655 HSCs with high expression of CD150 were significantly reduced compared to those with low
656 CD150 expression (Bars show mean with SD. Sidak's multiple comparison test: **p<0.01).
657

658 **Figure 4: Single hibernating HSCs can be manipulated by lentiviral transduction**

659 (A) CD45⁺EPCR⁺CD48⁻CD150⁺ (ESLAM) cells were isolated and transduced with ZsGreen
660 lentivirus and cultured together for 2 days in StemSpan supplemented with 10% FCS and IL-
661 11. Cells were collected and virus was removed by collecting and re-sorting the cells into
662 single wells and cultured in SCF-supplemented media for additional 10 days. 4001 total viable
663 cells (a mixture of transduced and non-transduced cells) were re-sorted and transplanted into
664 W41-CD45.1 (n=6 recipients) and donor contribution and GFP expression were assessed by
665 serial bleeds and flow cytometry analysis. (B) Graph shows the percentage of clones surviving
666 after 10 days post-addition of SCF, and the green bar indicated the percentage of GFP⁺ clones.
667 (C) and (D) Chimerism levels (20-40%) were stable across all recipients at all time points, and
668 an average of 1-2% of donor cells were positive for GFP at 16 weeks post-transplantation.
669 Bars show mean with SEM.

670

671 **Figure 5: Gene expression profiling reveals a common transcriptional program between**
672 **freshly isolated and hibernating HSCs**

673 (A) Uniform Manifold Approximation and Projection (UMAP) of single-cell RNA-seq
674 (scRNAseq) profiles derived from 4 distinct populations (HSC, blue dots; hibHSC, red dots;
675 HSC+SCF, green dots; hibHSC+SCF, orange dots). (B) The HSC-specific molecular overlap
676 (MoIO) gene signature score was computed based on average expression of signature genes
677 and projected onto the UMAP distribution. (C) MoIO scores for the individual HSCs in each
678 physiological state with the HSCs and hibHSCs having the highest overall scores. (D) Cell cycle
679 scores were computed for each cell and identified states were projected on the UMAP display

680 from 5D (G1(G0), pink; G2/M, orange; S, blue). (E) A proportional representation of cell cycle
681 stages of all cells within each distinct population (G1(G0), pink; G2/M, orange; S, blue). (F)
682 Heatmap of previously identified HSC-specific proliferation signature genes(Venezia *et al.*,
683 2004) sorted by cell type with low expression in HSCs and hibHSCs and high expression in both
684 sets of SCF stimulated cells.

685

686 **Figure 6: Hibernating HSCs have a unique molecular profile of stress response**

687 (A) Differential gene expression (DGE) was computed for two separate comparisons: (I)
688 comparison of fresh HSCs (HSC) against SCF-stimulated HSCs (HSC+SCF); (II) comparison of
689 hibernating HSC (hibHSCs) against hibHSCs post SCF-stimulation (hibHSC+SCF) (negative
690 binomial distribution, adjusted with Benjamini-Hochberg correction). Venn Diagrams
691 represent the number of genes commonly enriched in unstimulated populations (HSC and
692 hibHSC) and SCF-stimulated populations (HSC+SCF and hibHSC+SCF) from both separate DGE
693 computations. (B) Gene ontology (GO) term enrichment was computed based on
694 differentially expressed genes, as outlined in (A). Minimum *p-value* >0.05 to be considered
695 significantly enriched. (C) Volcano plot of differentially expressed genes (red dots), comparing
696 fresh HSCs (HSC) and hibernating HSCs (hibHSC) (negative binomial distribution, adjusted with
697 Benjamini-Hochberg correction). (D) Dot plot representing the average normalised expression
698 of genes across the 4 distinct populations. Genes of interest and MoLO signature genes were
699 selected from DGE in (C). The size of each dot indicates the proportion of cells with normalised
700 expression level >0 (scaled expression represented by colour intensity). (E) KEGG pathway
701 enrichment in unstimulated hibernating HSCs (hibHSC), showing selected metabolic and
702 signal transduction pathways (enrichment cut-off: adjusted *p-value* >0.05). (F) Violin plots of
703 normalised gene expression of selected differentially expressed genes, enriched in
704 unstimulated hibernating HSCs (hibHSCs).

705

706 **Figure 7: Hibernation conditions keep the majority of human HSCs as single cells**

707 (A) Single human HSCs (CD34⁺CD38⁻CD90⁺CD45RA⁻CD19⁻CD49f⁺) from umbilical cord blood
708 were sorted into individual wells and cultured in presence of IL-11 with or without SCF. In
709 parallel, human HSCs were bulk-cultured for 7 days in the absence of SCF and transplanted at
710 3 different cell doses (22, 110, and 218) into immunodeficient recipients and monitored for
711 engraftment. (B) Survival of HSCs in the presence or absence of SCF over 7 days, where

712 absence results in 1.5-fold reduced survival compared to SCF-supplemented cultures (fresh
713 n=192, post-hibernation n=672, 5 independent experiments). (C) The proportion of cells
714 divided at 5-7 days in culture with and without the addition of SCF is displayed. Significantly
715 more cells divide in the presence of SCF with the majority of cells in hibernation conditions
716 remaining as single cells (fresh, 3 independent experiments, post-hibernation, 5 independent
717 experiments). Bars show mean with SEM. (D) The graphs show the percentage of human cell
718 engraftment (%CD45⁺⁺) in PB from transplanted mice at 12- and 20-weeks post-
719 transplantation (cell dose 22, n=5; 110, n=4; 218, n=3). The threshold for events considered
720 as positive was >0.01% with a minimum of 30 analysed events. Non-engrafted mice shown
721 below dashed line. CD45⁺⁺ indicates cells positive for 2 distinct CD45 antibodies. Bars show
722 mean with SEM.

Figure 1

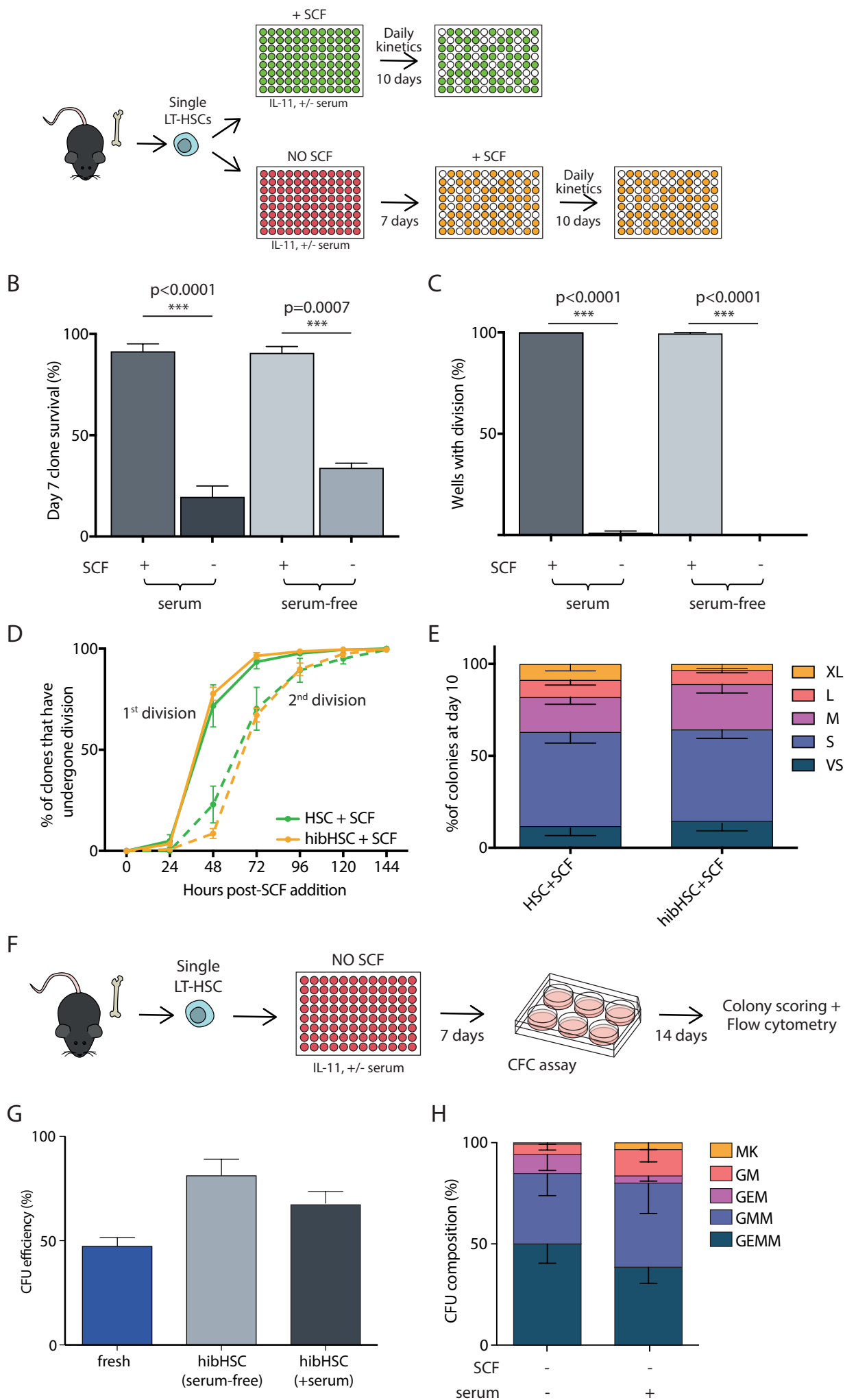


Figure 2

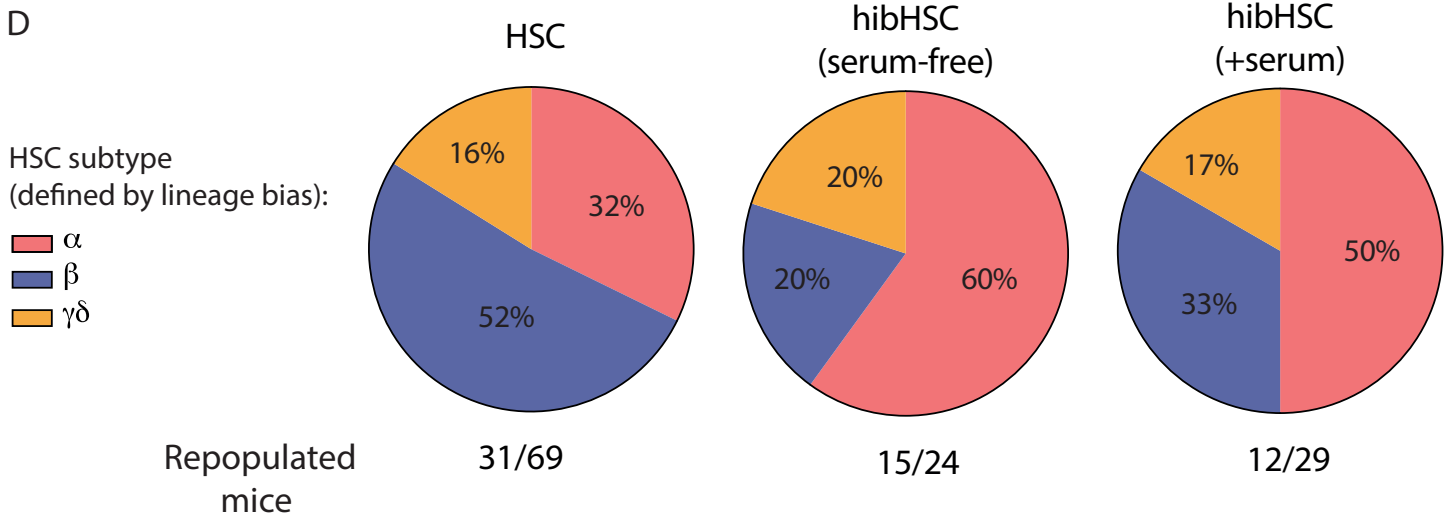
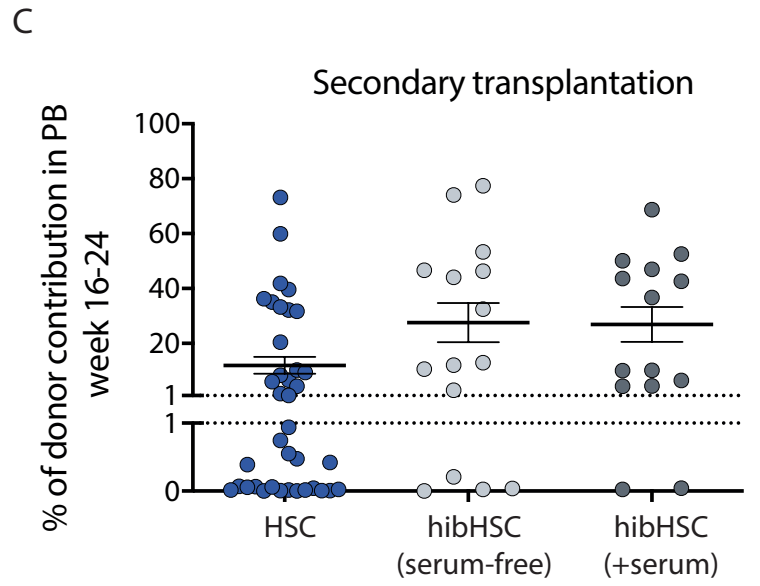
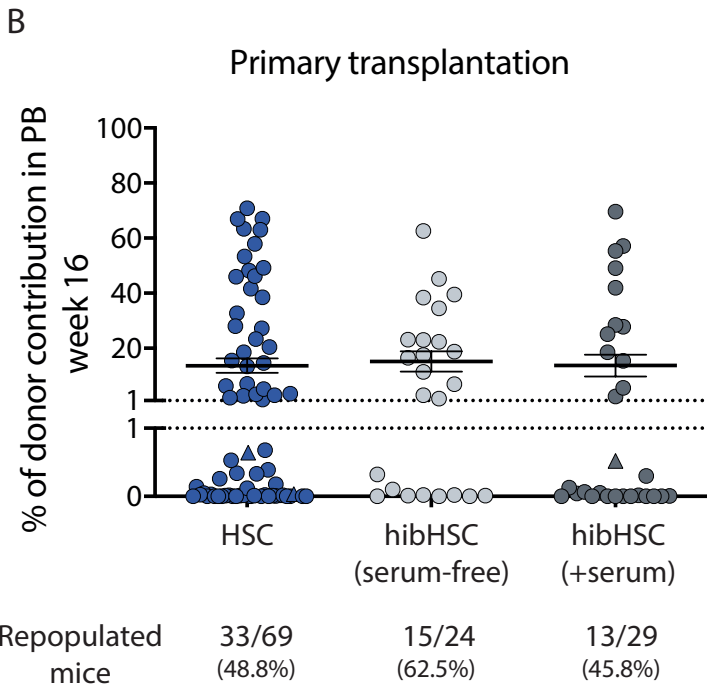
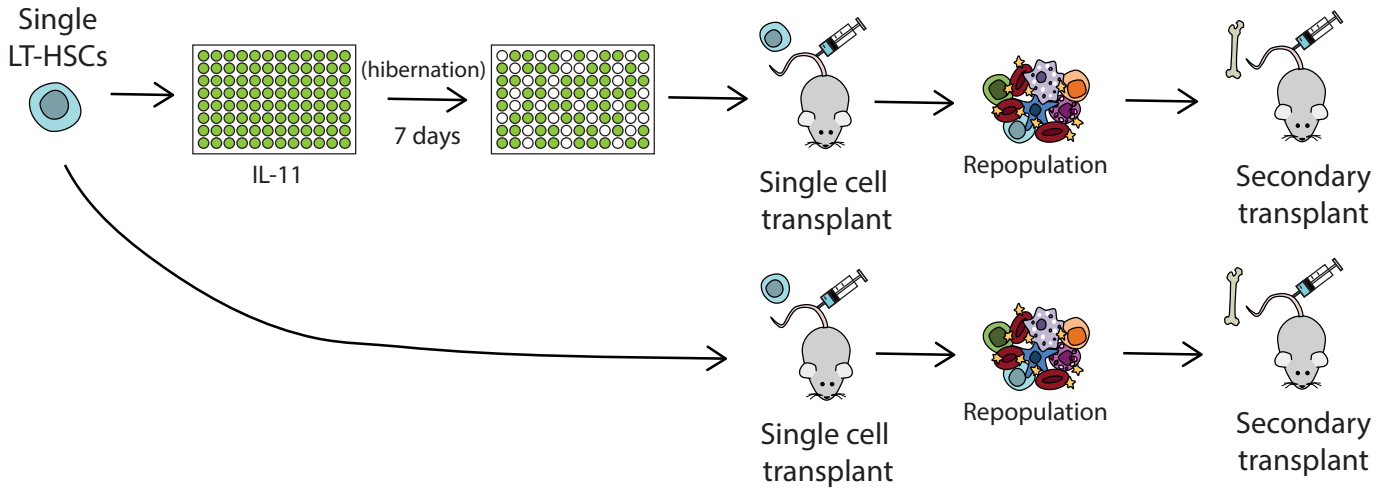
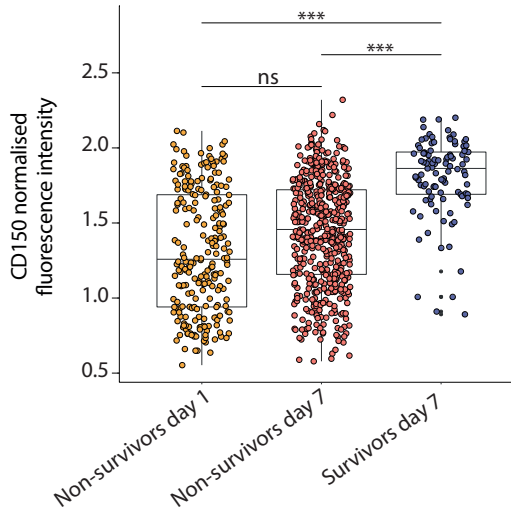
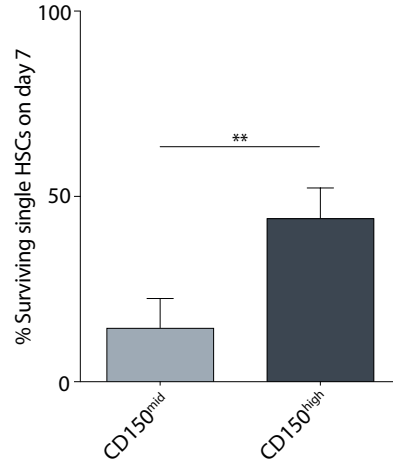


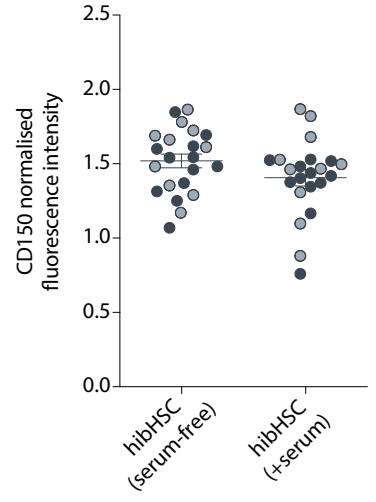
Figure 3



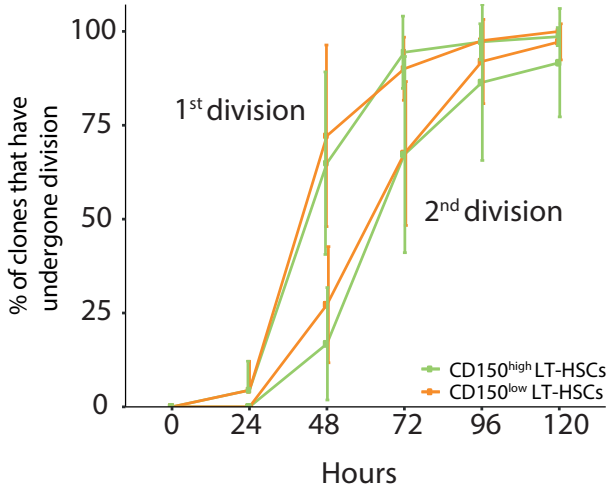
B



C



D



E

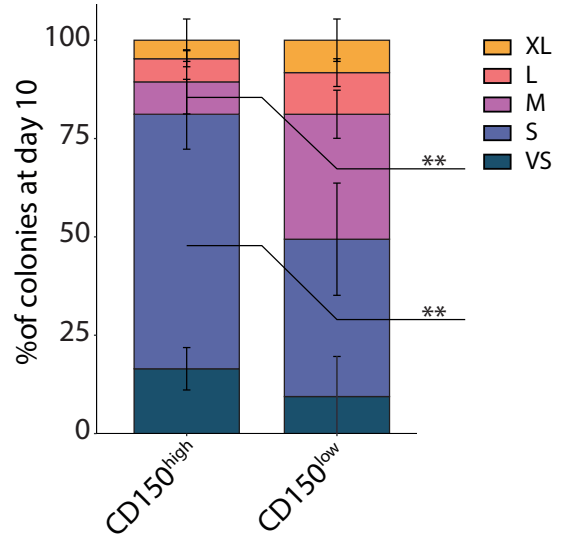
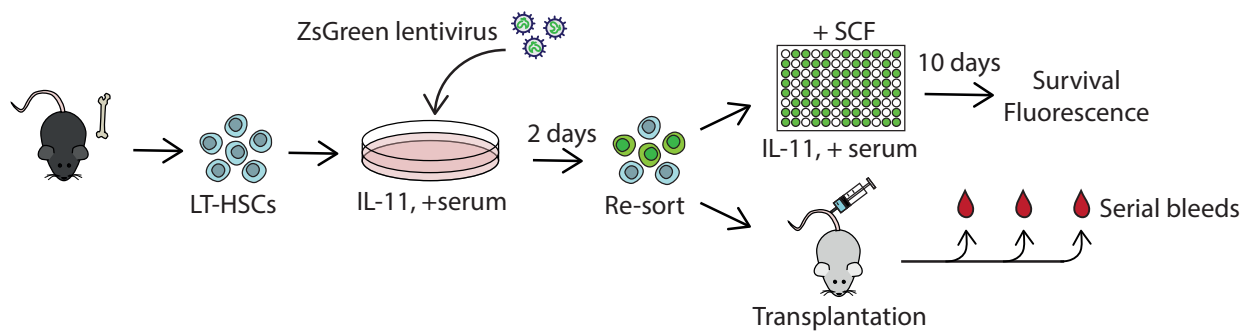
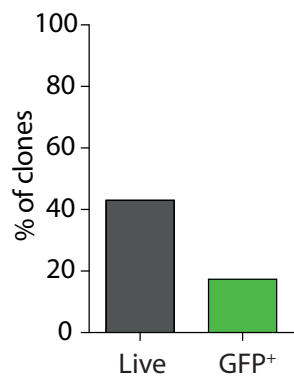


Figure 4

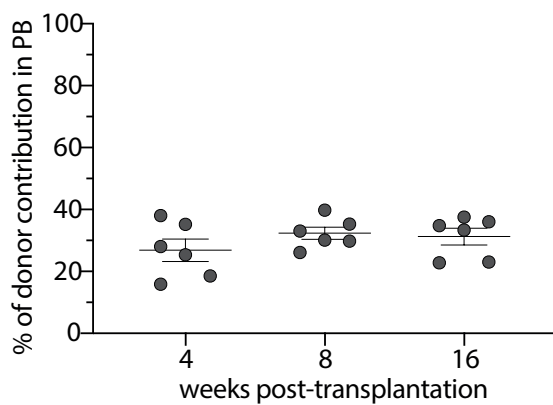
A



B



C



D

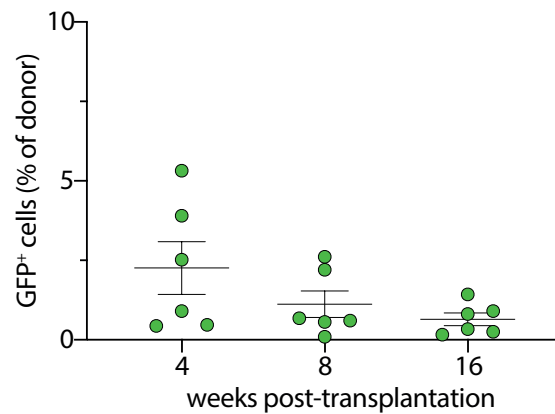


Figure 5

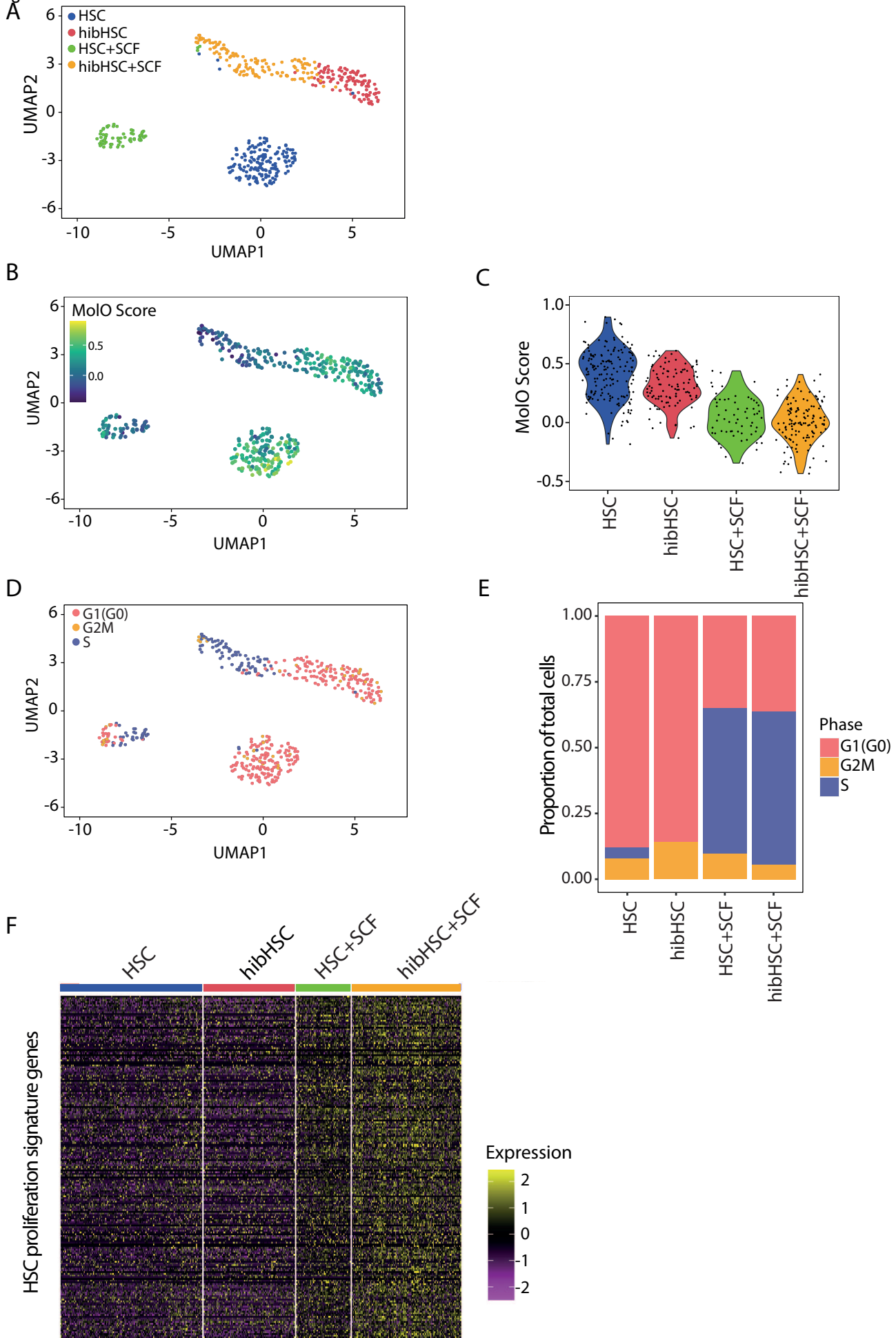


Figure 6

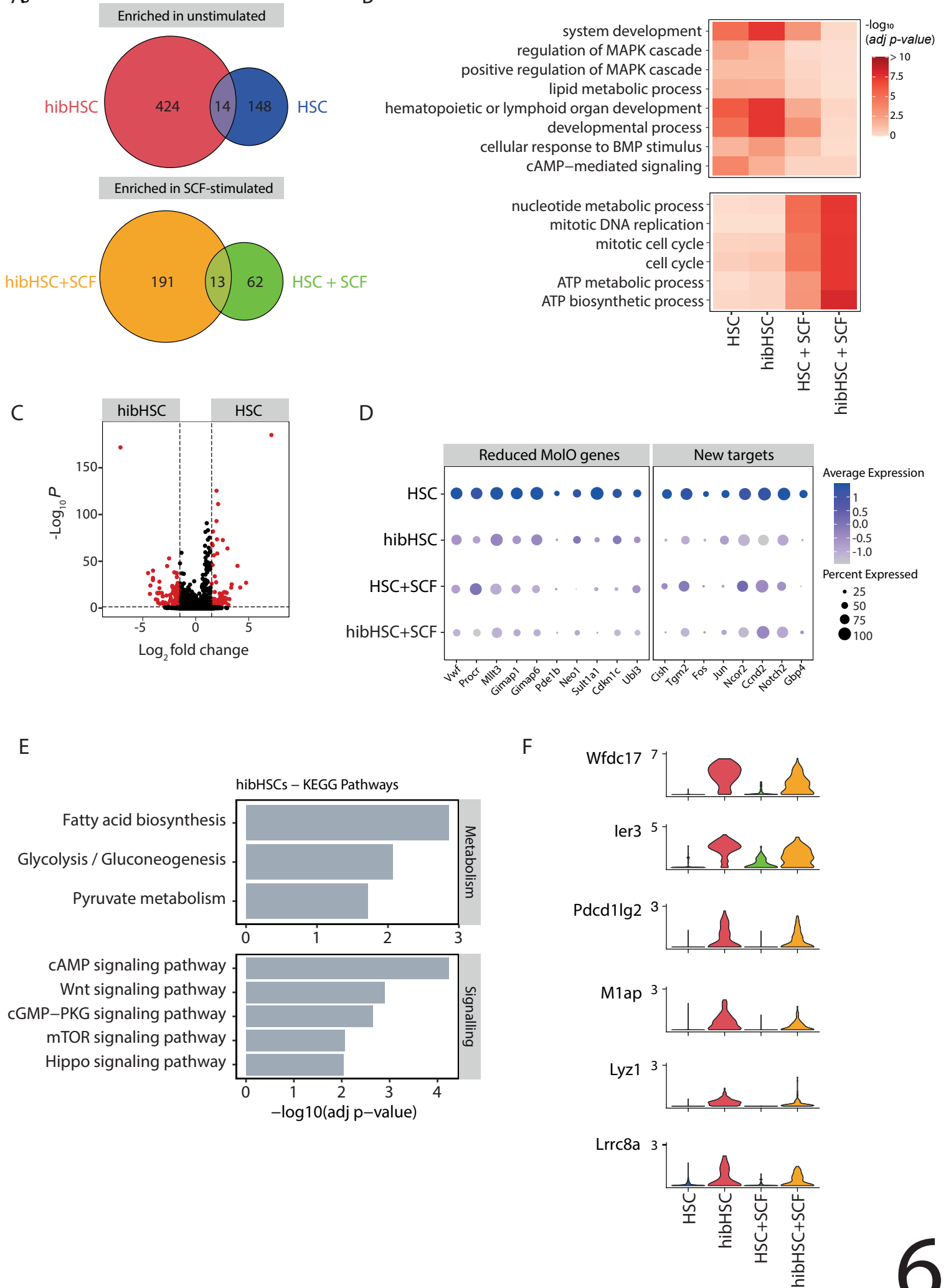
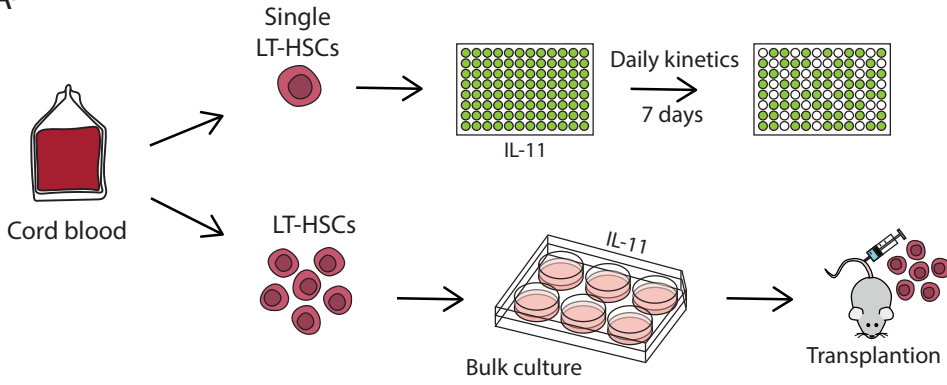
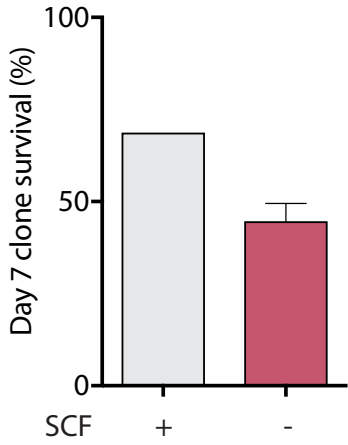


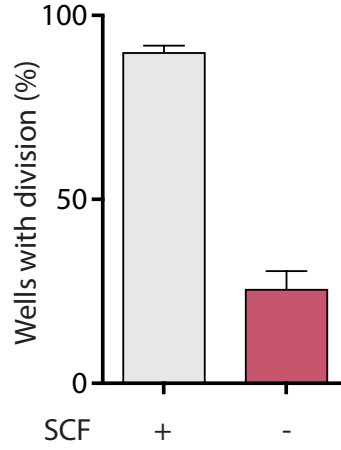
Figure 7



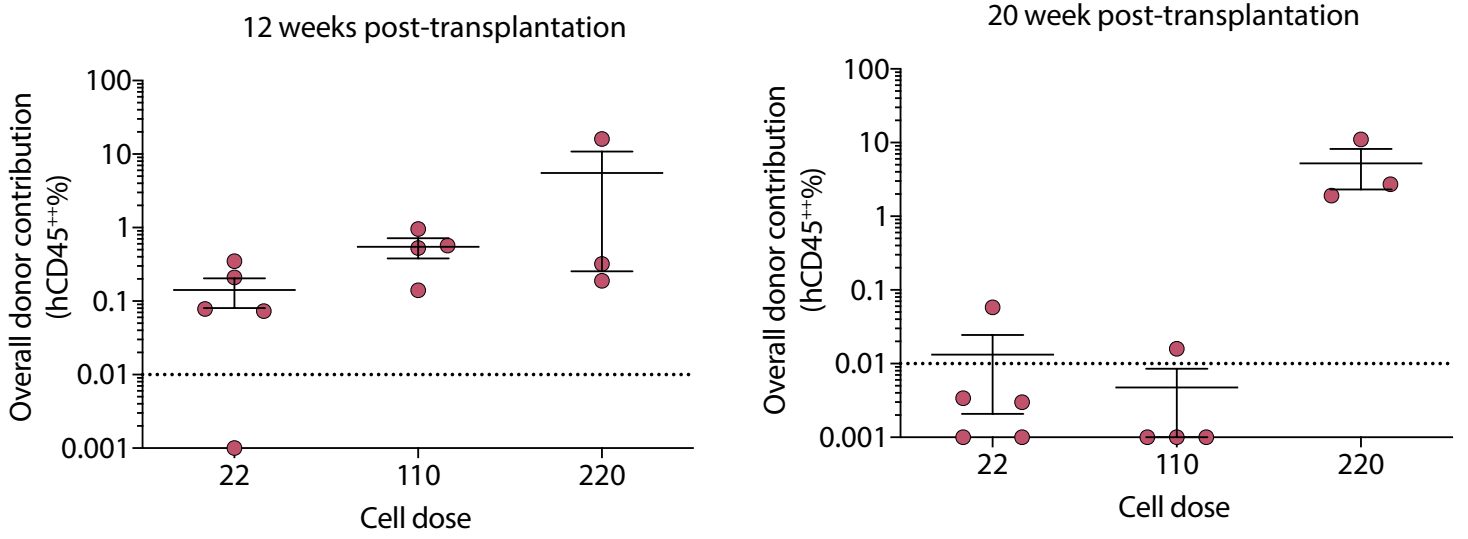
B



C



D



1 **Supplementary Data Items**

3 **Mice**

4 C57BL/6-Ly5.2 (WT) were purchased from Charles River Laboratory (Saffron Walden, Essex,
5 UK). C57BL/6w41/w41-Ly5.1 (W41) were bred and maintained at the University of
6 Cambridge. *NOD.Cg-Prkdc^{scid}Il2rg^{tm1Wjl}/SzJ* (NSG) mice were obtained from Charles River or
7 bred in-house. Mice were maintained in the Central Biomedical Service (CBS) animal facility
8 of Cambridge University and housed in specific pathogen-free environment, according to
9 institutional guidelines. All the procedures performed were in compliance with the guidance
10 on the operation of ASPA (Animals Scientific Procedures Act 1986), following ethical review
11 by the University of Cambridge Animal Welfare and Ethical Review Body (AWERB).

13 **Isolation of mouse Sca1^{high} ESLAM HSCs and *in vitro* assays**

14 Bone marrow cells were isolated from spine, sternum, femora, tibiae and pelvic bones of both
15 hind legs of WT mice. Bones were crushed in 2% Fetal Calf Serum (FCS, STEMCELL or Sigma
16 Aldrich (Sigma)) and 1mM EDTA (Sigma) in PBS (Sigma). Red cell lysis was performed by
17 treatment with Ammonium Chloride (NH₄Cl, STEMCELL). Depletion of mature lineage cells
18 was performed using EasySep mouse hematopoietic progenitor cell enrichment kit
19 (STEMCELL). HSCs were isolated from the lineage depleted cell suspension by using
20 fluorescence-activated cell sorting (FACS) using EPCR^{high}, CD45⁺, Sca-1^{high}, CD48^{low/neg}, CD150⁺
21 (or “ESLAM”), as described previously (Kent *et al.*, 2009), using CD45 FITC (Clone 30-F1,1 BD
22 Biosciences, San Jose CA, USA (BD)), EPCR PE (Clone RMEPCR1560, STEMCELL), CD150 Pacific
23 Blue (PB) or PE-Cy7 (Clone TC15-12F12.2, both from Biolegend, San Diego, USA (Biolegend)),
24 CD48 APC (Clone HM48-1, Biolegend), Sca-1 Brilliant Violet (BV) 421 (Clone D7, Biolegend)
25 and 7-Aminoactinomycin D (7AAD) (Life Technologies, Carlsbad, CA, USA (Life Technologies)).
26 The cells were sorted in either purity or single sort mode on an Influx cell sorter (BD
27 Biosciences, San Jose, CA, USA (BD)) using the following filter sets 488 530/40 (for FITC), 561
28 585/29 (for PE), 405 460/50 (for BV421), 640 670/30 (for APC), 561 750LP (for PE/Cy7), 640
29 750LP (for APC/Cy7), 405 520/35 (for BV510), 640 720/40 (for AF700), and 561 670/30 (for 7-
30 AAD) or 405 450/50 (for DAPI). When single HSCs were required, the single-cell deposition
31 unit of the sorter was used to place 1 cell into each well of a round bottom 96-well plate, each

32 well having been preloaded with 50uL medium which would be topped up with 50uL medium
33 with 2X cytokines.

34

35 **Normalisation of single cell index-sorting data**

36 Surface marker intensity of single ESLAM HSCs across experiments were normalised and batch
37 corrected by using the flowCore (version 1.42.3) and sva (version 3.24.4) R packages. HSCs
38 were sorted in 96-well format and each plate was considered as an independent batch prior
39 to batch correction. All recorded surface markers were arranged in a flow frame and subject
40 to logicle transformation prior to batch correction. The analysis was computed in R (version
41 3.4.2) and performed by Daniel Bode. The original script was developed by Blanca Pijuan Sala.

42

43 **Liquid cultures and clone size determination of mouse HSCs**

44 Single HSCs were sorted and cultured into 100µL StemSpan SFEM (STEMCELL) supplemented
45 with 300 ng/mL SCF (R&D Systems, Bio-Techne, Minneapolis, MI, USA, (R&D)), 20ng/mL
46 human Interleukin-11 (IL-11, R&D), 2 mM L-Glutamine (Sigma), 1000 U/mL-100 µg/mL
47 Penicillin-Streptomycin (Sigma), 100µM 2-Mercaptoethanol (Life Technologies). SCF
48 concentration was 300ng/mL unless stated otherwise. 10% of FCS was supplemented when
49 stated. For serum-free cultures, cells were sorted into Ham's F12 nutrient mixture (Gibco,
50 ThermoFisher, Waltham, MA, USA (Gibco)) supplemented with 20 ng/mL human IL-11 (R&D),
51 300 ng/mL SCF (SCT or R&D), 2 mM L-Glutamine (Sigma), 1000U/mL-100 µg/mL Penicillin-
52 Streptomycin (Sigma), 1% ITS-X (Insulin-Transferrin Selenium-Ethanolamine, Gibco), 100 mM
53 HEPES (4-(2-hydroxyethyl)-1 piperazineethanesulfonic acid, Sigma), 100 mg/mL human serum
54 albumin (HSA, Albumin Bioscience, Huntsville, AL, USA).

55 Cells were cultured at 37°C, 5% CO₂, 20% O₂. Cell counts were performed every 22-24 hours
56 and cell cycle kinetics determined for the first and second division by visual inspection, scoring
57 wells as having 1, 2, or 3-4 cells. Clone size at day 10 post-isolation was scored as very small
58 (less than 50 cells), small (50-500 cells), medium (500-10,000 cells), or large (10,000 or more
59 cells).

60

61 **Time lapse of single mouse HSCs**

62 Single cells were sorted into a 96 well plate and imaged on a Leica DMI3000 B microscope,
63 housed inside an Okolab CO2 microscope cage incubator system. Custom written LabVIEW
64 software was used to control a Prior Proscan III nanopositioning stage and acquire images via
65 a Hamamatsu Orca Flash 4.0 camera. Cells were imaged every 50 minutes for the first 7 days,
66 the fastest time resolution achievable with the system while allowing enough time for the
67 autofocus routine to correctly execute at all 96 wells. On day 7, the plate was removed and
68 300ng/mL SCF was added to the 67 wells where there was a possibility of a viable cell,
69 determined by eye. The reduction in well number allowed for an increase in time resolution
70 to 35 minutes. By day 11, imaged well number was further reduced to 17 wells as it became
71 more apparent in which wells cells were still viable. This allowed for a corresponding increase
72 in time resolution to 20 minutes. Imaging continued until day 14.

73

74 **Colony-forming assays of mouse HSCs**

75 Single cultured cells (hibernated HSCs) were transferred from liquid culture into 600 μ l of
76 MethoCult GF M3434 (STEMCELL). Freshly isolated HSCs were isolated by FACS sorting (as
77 described above) and plated into 3 mL Methocult GF M3434 (STEMCELL) and split across 2
78 wells of 6-well plates. Cells were cultured for 14 days and colony number was assessed by
79 visual inspection and colony type scored by antibody staining with CD41 FITC (Clone
80 MWReg30), CD61 PE (Clone 2C9.G2 (HM β 3-1), Ter119 PE-Cy7 (Clone TER-119), CD45.2 APC-
81 Cy7 (Clone 104), Ly6G/Gr1 BV421 (Clone 1A8), CD11b/Mac1 APC (Clone M1/70). Samples
82 were acquired on LSR Fortessa (BD) and flow cytometry data analysing by using FlowJo
83 (Treestar, Ashland, OR, USA).

84

85 **Bone Marrow Transplantation Assay and Peripheral Blood Analysis**

86 Donor cells were obtained from C56BL/6J mice (CD45.2). Recipient mice were
87 C57Bl6W41/W41 (W41) mice as described previously (Kent *et al.*, 2009; Benz *et al.*, 2012).
88 Recipient mice were sub-lethally irradiated with a single dose (400cGy) of Cesium irradiation
89 and all transplants were performed by intravenous tail vein injection using a 29.5G insulin
90 syringe. Single HSCs were deposited by FACS into 100 μ L of medium in a 96-well U-bottom
91 plate. All liquid was subsequently mixed with extra 100 μ L of PBS and aspirated into the insulin
92 syringe (avoiding air bubbles) and injected into the tail vein. For secondary transplantations,
93 whole bone marrow was obtained from primary recipient by flushing tibiae and femurs with

94 PBS + 2%FCS. Red cell lysis was performed and an equivalent of one femur ($\sim 2 \times 10^7$ cells) of
95 each donor mouse was transplanted into at least two secondary recipients.

96

97 PB samples were collected in EDTA coated microvette tubes (Sarstedt AGF & Co, Nuembrecht,
98 Germany). Blood was collected from the tail vein at week 8, 12, 16, 20, 24, post-
99 transplantation, unless otherwise stated. Red cell lysis was performed by using NH_4Cl and
100 samples were subsequently analysed for repopulation levels as previously described (Kent et
101 al. 2016; Wilson et al. 2015). Cells were stained for lineage markers using Ly6g BV421 (Clone
102 1A8), B220 APC (Clone RA3-6B2), CD3e PE (Clone 17A2), CD11b/Mac1 PE-Cy7 or BV605 (Clone
103 M1/70), CD45.1 AF700 (Clone A20), CD45.2 FITC (Clone 104). All antibodies were obtained
104 from Biolegend. Samples were acquired on LSR Fortessa (BD) and flow cytometry data
105 analysing by using FlowJo (Treestar, Ashland, OR, USA).

106

107 **Single cell RNA sequencing analysis**

108 Single cell RNA sequencing (scRNA seq) analysis was performed as described previously in
109 Picelli et al. 2014 (Smart-seq2). Single ESLAM HSCs were sorted by FACS into 96-well PCR
110 plates containing lysis buffer (0.2% Triton X-100 (Sigma), RNase inhibitor (SUPERase,
111 ThermoFisher), nuclease-free water (Thermo Fisher)) Illumina Nextera XT DNA preparation kit
112 was used to prepare the libraries, which were pooled and run on the Illumina Hi-Seq4000 at
113 the CRUK Cambridge Institute Genomics Core. Cells from which low-quality libraries with
114 insufficient sequencing depths were generated were excluded by setting the threshold of
115 number of mapped reads to $> 2 \times 10^5$, with mapped reads comprising nuclear genes,
116 mitochondrial genes and ERCCs. A minimum threshold of 20% for reads mapping to known
117 genes was set, in order to exclude empty wells and dead cells. In addition, the threshold for
118 reads mapping to mitochondrial genes was > 0.2 , to ensure a minimum of 20% of reads to map
119 to non-mitochondrial genes. Protein-coding genes were extracted for further processing. GEO
120 accession number: GSE160131.

121

122 **Lentiviral transduction of mouse HSCs**

123 7000 ESLAM HSCs cells were isolated and split between 4 wells (1750 cells/well) of a 96-well
124 plate (Corning). Following their isolation, cells were kept in 50 μL of medium (StemSpan,
125 10%FCS, 20ng/mL IL-11) and were supplemented with polybrene (Sigma) and pHIV-ZsGreen

126 CSTVR lentivirus supplied by Dr Alasdair Russell from Cancer Research UK (CRUK). Plates were
127 centrifuged at 600g for 30 minutes, at 30°C, to promote infection, before being transferred
128 into a 37°C incubator. Two days after, cells were collected from the wells and resorted for
129 viability (7AAD-). Live cells (4001) were transplanted into 6 sub-lethally irradiated CD45.1 W41
130 recipient mice (for an approximate dose of 615 cells/mouse) and monitored for donor
131 chimerism as described above, and GFP expression.

132

133 **Isolation of human CB HSCs and *in vitro* assays**

134 Cord blood samples were obtained from Cambridge Blood and Stem Cell Biobank (CBSB) with
135 informed consent from healthy donors in accordance with regulated procedures approved by
136 the relevant Research and Ethics Committees. Mononuclear cells (MNCs) were isolated using
137 Lymphoprep (Axis Shield PLC, Dundee, UK) or Pancoll lymphocyte separating medium
138 (Pancoll, PAN Biotech, Aidenbach, Germany). Blood was mixed with equal volume of PBS and
139 layered on Lymphoprep/Pancoll. Layered blood was centrifuged at 1400 rpm for 25 min, at
140 room temperature with the brake off. The MNC layer was carefully aspirated and washed with
141 PBS, to remove any separating medium trace. Red cell lysis was subsequently performed by
142 using red cell lysis buffer (Biolegend, San Diego, CA, USA (Biolegend)). MNCs were depleted
143 of differentiated hematopoietic cells by using the human CD34 microbead kit (Miltenyi Biotec,
144 Bergisch Gladbach, Germany) with the following modifications: all cells were resuspended in
145 90 μL PBS, 2% FCS / 10^8 cells, CD34 Microbeads were used at
146 30 $\mu\text{L}/10^8$ cells and FcR Blocking Reagents at 30 $\mu\text{L}/10^8$ cells. Cells were separated using
147 the AutoMACS cell separation technology (Miltenyi Biotec).

148 CD34 enriched cells were stained with CD34 APC-Cy7 (Clone HIT2, Biolegend), CD38 PE-Cy7
149 (Clone HIT2, Biolegend), CD45RA FITC or PE (Clone HI100, Biolegend), CD90 APC or PE (Clone
150 5E10, Biolegend or Biosciences respectively), CD49f PE-Cy5 (Clone GoH3, Biosciences) and
151 Zombie Aqua (Biolegend) was used as a cell viability marker. HSCs were sorted as CD34⁺,
152 CD38⁻, CD45RA⁻, CD19⁻, CD49f⁺, CD90⁺ on a BD FACS Aria fusion sorter at the NIHR Cambridge
153 BRC Cell Phenotyping Hub facility. The single cells were sorted into individual wells of a 96-
154 well U-bottom plate, each well having been preloaded with 100 μL medium.

155

156 **Liquid cultures and clone size determination of human LT-HSCs**

157 Single HSCs were sorted into 96-well U-bottom plates and cultured in 100µL StemSpan SFEM
158 (STEMCELL) supplemented with 100 units/mL Penicillin and 100µg/mL Streptomycin
159 (Pen/Strep, Sigma-Aldrich), 2mM L-Glutamine (Sigma-Aldrich), 10⁻⁴M 2-Mercaptoethanol and
160 20 ng/mL IL-11 (Biotechne, Abingdon, UK (Bio-techne)), 300ng/mL stem Cell Factor (SCF,
161 R&D)(added when specified), 10% FCS (added when specified). Cell survival was assessed by
162 visual inspection on day 10 (the sorting day is determined as day 0).

163

164 **Xenotransplantation and Peripheral Blood Analysis**

165 10,862 LT-HSCs were isolated from CD34 enriched CB and cultured into a single well (U-
166 bottom 96-well plate) for 7 days as described above for the single cell culture. On day 7, cell
167 number was assessed by visual inspection and cells were serially diluted in PBS as following:
168 ~110 cells split into 5 recipients (~22 cell per mouse), ~440 cells split into 4 recipients (~110
169 cells per mouse), ~654 cells split into 3 recipients (~218 cells per mouse). NSG mice were sub-
170 lethally irradiated with a single dose (2.4 Gy) by Cesium irradiation. Twenty-four hours later
171 mice were anesthetised with isoflurane and injected intrafemorally as previously described
172 ²⁹.

173 PB samples were collected in EDTA coated microvette tubes (Sarstedt AGF & Co, Nuembrecht,
174 Germany). Blood (~100µL) was collected from the tail vein at 8, 12, and 20 weeks post-
175 transplantation. Mice were sacrificed 20 weeks post-transplantation and BM cells were
176 isolated by flushing the injected femur with PBS/FCS. Blood was transferred into polystyrene
177 tubes (Becton Dickinson) tubes and diluted 1:1 with 2%FCS in PBS. 1 mL of Lymphoprep
178 (STEMCELL) was carefully layered at the bottom of the tube and the tubes were centrifuge
179 for 25 min at 500g (brake off). MNCs were collected, washed with PBS and resuspended in
180 50µL of PBS/FCS and transferred into a 96 u-bottom plate (Falcon) to stain. Cells were stained
181 with the following lineage markers: CD19/FITC (clone HIB19, Biolegend), GlyA/PE (clone HIR2,
182 BD), CD45/PE-Cy5 (clone HI30, Biolegend), CD14/PE-Cy7 (clone M5E2, Biolegend), CD33/APC
183 (clone P67.6, BD), CD19/AF700 (clone HIB19, Biolegend) , CD3/APC-Cy7 (clone HIT3a,
184 Biolegend), CD45/BV510 (clone HI30, Biolegend). Samples were acquired on LSR Fortessa (BD)
185 and flow cytometry data were analysed by using FlowJo v10 (FLOWJO LLC, Ashland, OR, USA).
186 To detect human engraftment, two distinct antibodies against CD45 were used, and cells were
187 considered human if positive for both (CD45⁺⁺). Mice were considered successfully

188 repopulated if the percentage of (CD45⁺⁺) \geq 0.01% (and at least 30 cells were recorded in
189 these gates).

190

191 **Statistical analysis**

192 Computational analyses were performed in the R programming environment (version 3.6.3).
193 Raw data was processed using the Seurat tool (version 3.2.0)(Butler *et al.*, 2018; Stuart *et al.*,
194 2019). The recommended standard processing pipeline was applied to perform log-
195 normalisation (default settings) and identify highly variable genes (nfeatures=10,000).
196 Subsequently, expression values were scaled using default parameters. Dimensionality
197 reduction, including principal component analysis (PCA) and Uniform Manifold
198 Approximation and Projection (UMAP) was performed using default Seurat tools. Differential
199 gene expression was performed using negative binomial generalised linear models, as
200 implemented by DESeq2 (version 1.26.0)(Love, Huber and Anders, 2014). Genes with adjusted
201 *p-value* <0.05 and logFC >1.5 were considered significantly differentially expressed
202 (Benjamini-Hochberg corrected). Cell cycle scoring was performed based on average
203 expression of key cell cycle genes, as described previously(Tirosh *et al.*, 2016). Similarly, gene
204 set scoring was computed for previously described HSC proliferation quiescence signatures
205 (Venezia *et al.*, 2004). Such scoring was also applied to gene sets, previously identified as
206 upregulated and downregulated in cells in a G0 state(Cheung and Rando, 2013). Batch effect
207 testing and correction was performed to inform any potential influence of technical bias.
208 Normalisation and variable gene scoring were computed for each batch separately, using
209 variance stabilising transformation. Subsequently, separate batches were integrated using
210 canonical correlation analysis (CCA) by computing integration anchors (parameters: dims =
211 1:30 and k.filter = 10)(Stuart *et al.*, 2019). A very limited batch correction was identified
212 between Day 1 and Day 2 batches (Supplementary figure 1B). However, full data integration
213 introduced extensive over-correction and downstream analysis was performed without batch
214 correction (data not shown). All data visualisation was computed in R. To inspect downstream
215 IL-11 signalling, the following curated pathways gene sets, as outlined in the gene set
216 enrichment analysis database (Mootha *et al.*, 2003; Subramanian *et al.*, 2005) were retrieved:
217 I) KEGG_JAK_STAT_SIGNALING_PATHWAY (M17411); II) BIOCARTA_NFKB_PATHWAY
218 (M15285); III) HALLMARK_PI3K_AKT_MTOR_SIGNALING (M5923);
219 KEGG_MAPK_SIGNALING_PATHWAY (M10792). Similarly,

220 KEGG_REGULATION_OF_AUTOPHAGY (M6382) and REACTOME_CELLULAR_SENESCENCE
221 (M27188) were used. All gene sets were subsequently manually curated to exclude ligand and
222 receptor-associated genes (Supplementary Table 1).

223 To compute gene ontology (GO) and KEGG pathway enrichment, gene symbols were
224 converted to Entrez gene identifiers, using the mouse genome annotation database
225 (org.Mm.eg.db, version 3.10.0). GO terms were extracted from the GO annotation database
226 (GO.db, version 3.10.0). GO term enrichment and KEGG pathways analysis was computed
227 using the Limma package (version 3.42.2). An adjusted *p-value* < 0.05 cutoff was set to
228 determine GO term or KEGG pathway enrichment. Genes identified as significantly
229 differentially expressed between cell types were used conduct pathway enrichment.

230 Gene set enrichment analysis (GSEA) was performed using the UC San Diego-Broad Institute
231 GSEA software (version 4.0.3) (Mootha *et al.*, 2003; Subramanian *et al.*, 2005). Pre-ranked
232 gene lists were computed based on differentially expressed genes. GSEA was computed using
233 multiple databases, including GO biological processes, KEGG pathways and the Reactome
234 database. Analysis parameter were set as follows: 1000 permutations, weighted enrichment,
235 minimum 15 and maximum 500 genes annotated to gene set.

236

237 **Supplementary appendix 1: Single-cell time-lapse imaging of single HSCs in hibernation**
238 **cultures.**

239

240 **Supplementary table 1: JAK/STAT, MAPK, NFKB, PI3K/AKT gene sets**

241 JAK/STAT, MAPK, NFKB, PI3K/AKT gene sets manually curated to exclude ligand- and receptor-
242 associated genes. See also Supplementary Figure 1.

243

244 **Supplementary Figure 1: Molecular profiling of HSC, hibHSC, HSC+SCF, hibHSC+SCF, related**
245 **to Figure 5**

246 (A) UMAPs depicting (I) cell type (HSC, blue dots; hibHSC, red dots; HSC+SCF, green dots;
247 hibHSC+SCF, orange dots); (II) batches (batch 0, orange dots; batch 1, blue dots; batch 2,
248 green dots; batch 3, pink dots); days batches were sequenced (day 1, purple dots; day 2, blue
249 dots; day 3, orange dots). (B) MoIO gene relative expression in HSC, HSC+SCF, hibHSC,
250 hibHSC+SCF (C) Left panel, PCA of all cells coloured by computationally assigned cell cycle

251 category, right panel, the 4 cellular states are projected onto the PCA. The PCA was computed
252 using cell cycle genes exclusively.

253

254 **Supplementary Figure 2: HSC proliferation and quiescence signature genes, related to**
255 **Figure 5**

256 (A) Violin plots displaying individual proliferation scores by physiological condition (B) Gene
257 Set Enrichment Analysis of the HSC proliferation signature (Venezia *et al.*, 2004), computed
258 using DE genes of direct comparison of HSCs and HSC+SCF. (C) Heatmap of previously
259 identified HSC-specific quiescence signature genes (Venezia *et al.*, 2004), sorted by cell type.
260 (D, E) Gene sets upregulated in G0 cell populations and gene sets downregulated (anti-G0)
261 were used to compute G0 and anti-G0 gene signature scores (Cheung and Rando, 2013).
262 These were projected onto the UMAP depictions (see Figure 5A or Supplementary Figure 1A
263 for reference).

264

265 **Supplementary Figure 3: Autophagy, senescence, and IL-11RA gene signatures, related to**
266 **Figure 5**

267 (A) Autophagy gene signature scores projected onto the UMAP landscape and summarised in
268 form of a violin plot. (B) Senescence gene signature depicted as described in (A). (C) Violin
269 plot of the IL-11 receptor gene (IL-11RA1) and gene signature scores for core signalling
270 pathways stimulated by IL-11. Includes: PI3K, NKFB, MAPK and JAK-STAT. (D) Violin plots of
271 top differentially expressed PI3K pathway genes. (E) Top differentially expressed genes of the
272 NF-kB pathway.

273

274 **Supplementary Figure 4: Specific gene sets are altered during hibernation and SCF-**
275 **stimulation, related to Figure 6**

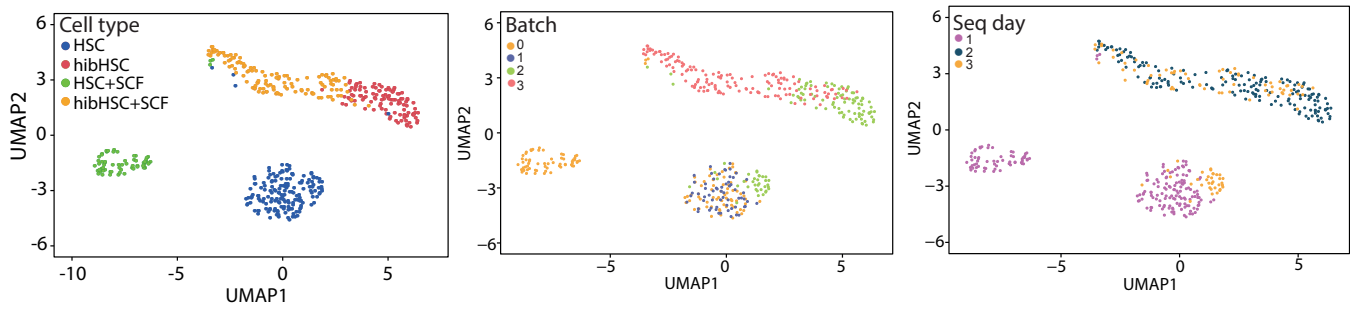
276 (A) Violin plots of normalised gene expression of the 13 upregulated genes in SCF-stimulated
277 cells (HSC+SCF, hibHSC+SCF). (B) Volcano plot of differentially expressed genes, comparing
278 HSCs and hibHSC. DE genes are marked in red ($\log_{2}FC > 1$ and $adj\ p\text{-value} < 0.05$, Benjamini-
279 Hochberg corrected). (C) Violin plots of normalised gene expression of genes of interest,
280 downregulated in hibHSC compared to HSC.

281

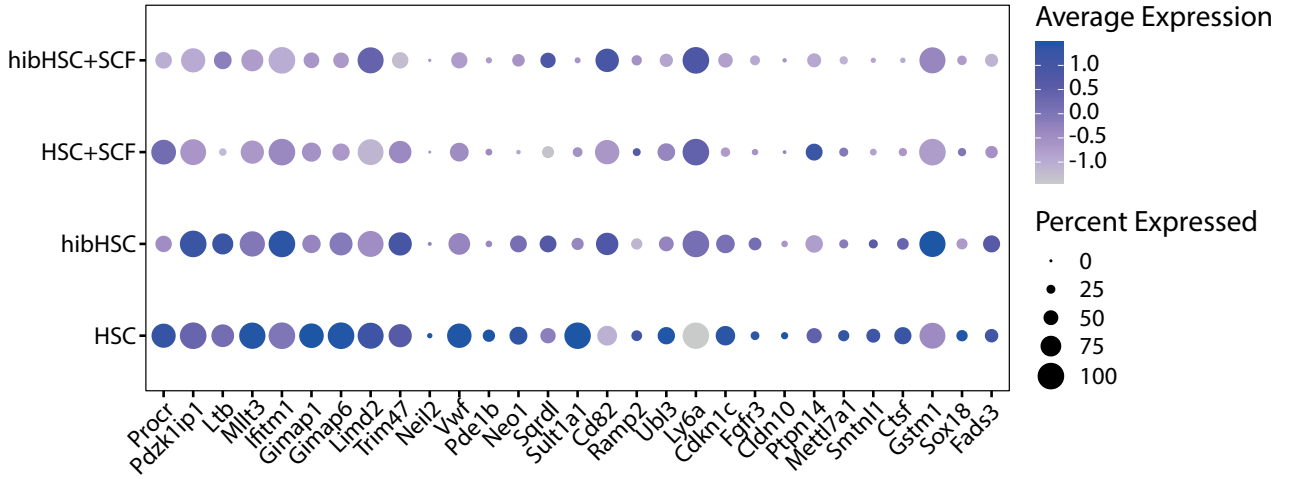
282 **Supplementary Figure 5: Genes of interests enriched in hibHSCs, related to Figure 6**

283 UMAPs of selected genes of interests enriched in hibHSC (manually selected from DE gene
284 set. The large majority of the hibHSCs appear in the upper right portion of the plot (see Figure
285 5A or Supplementary Figure 1A for reference).

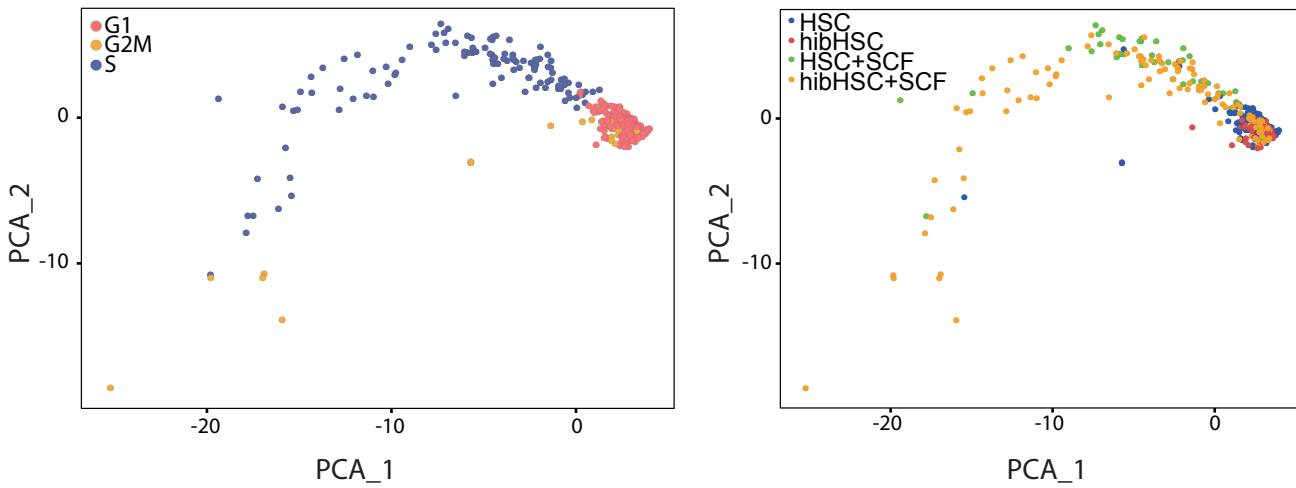
A



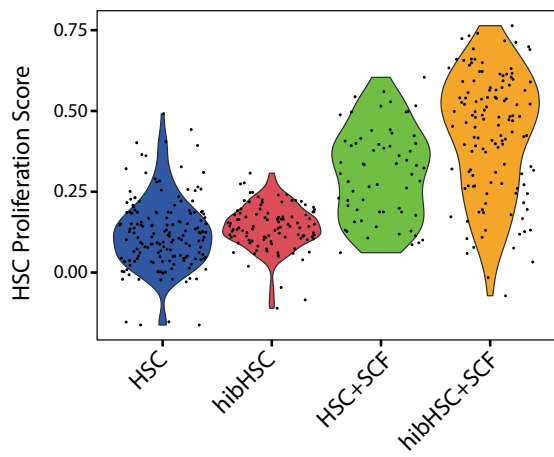
B



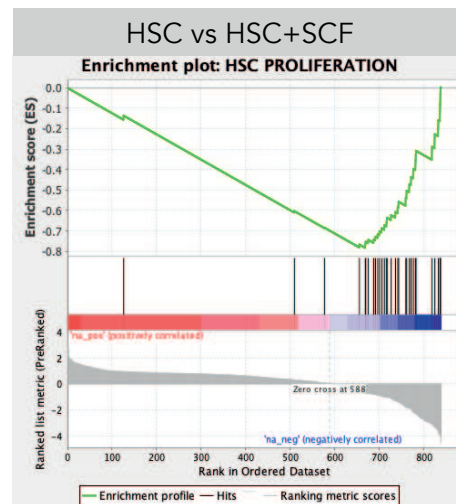
C



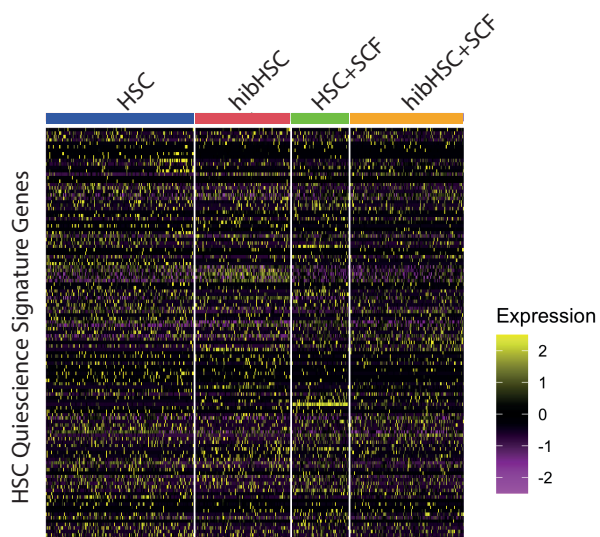
A



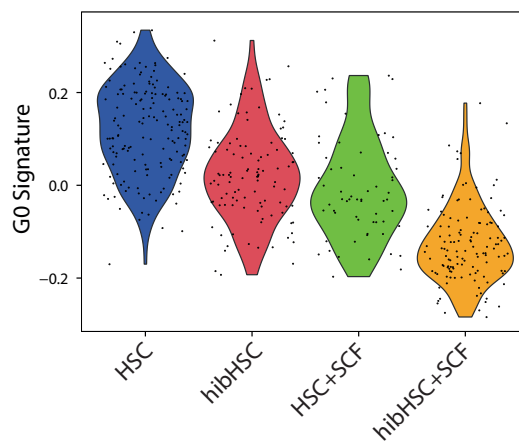
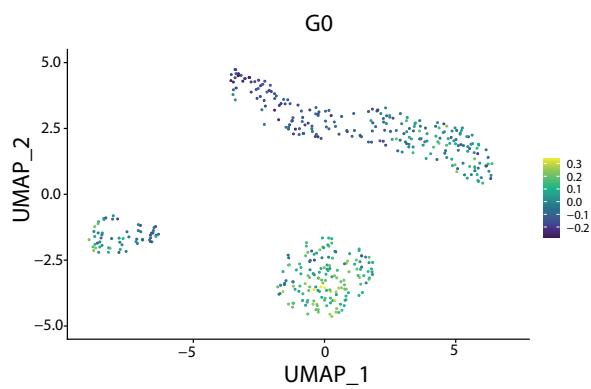
B



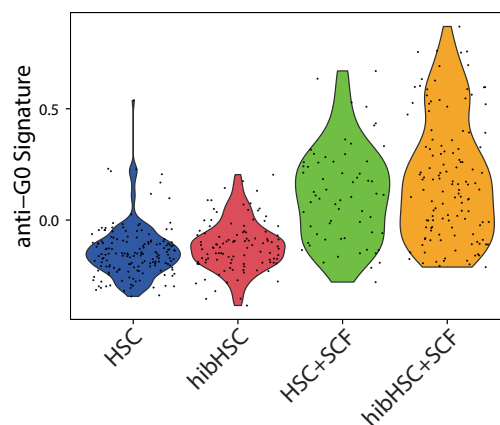
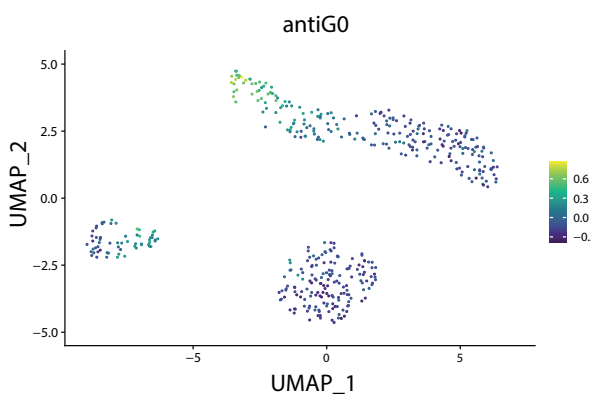
C



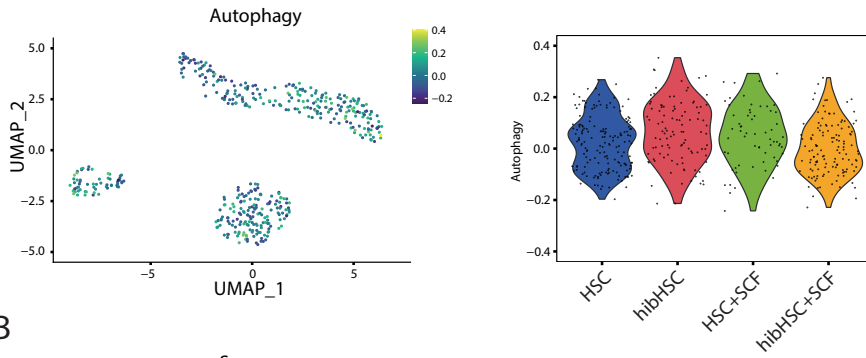
D



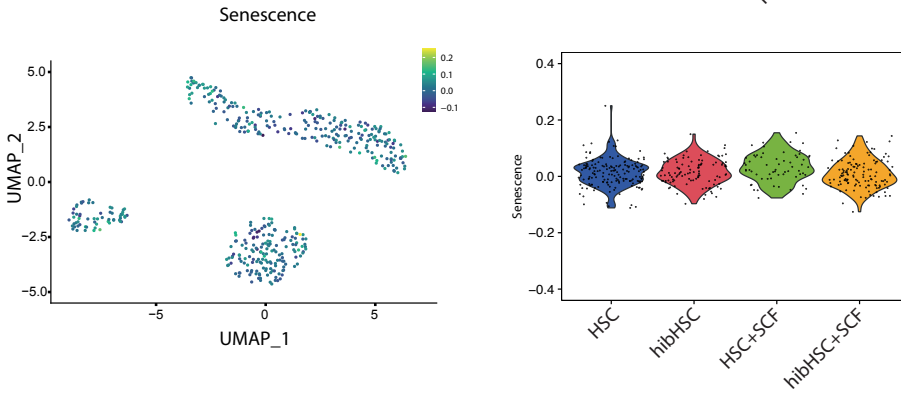
E



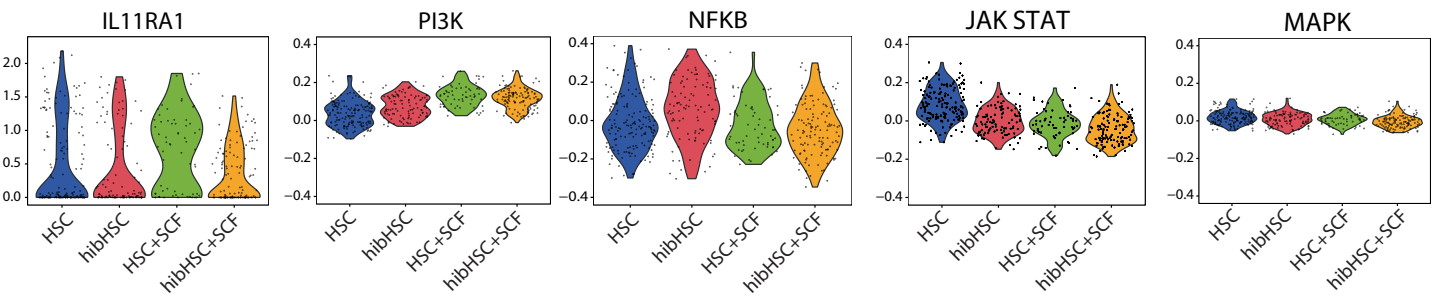
A



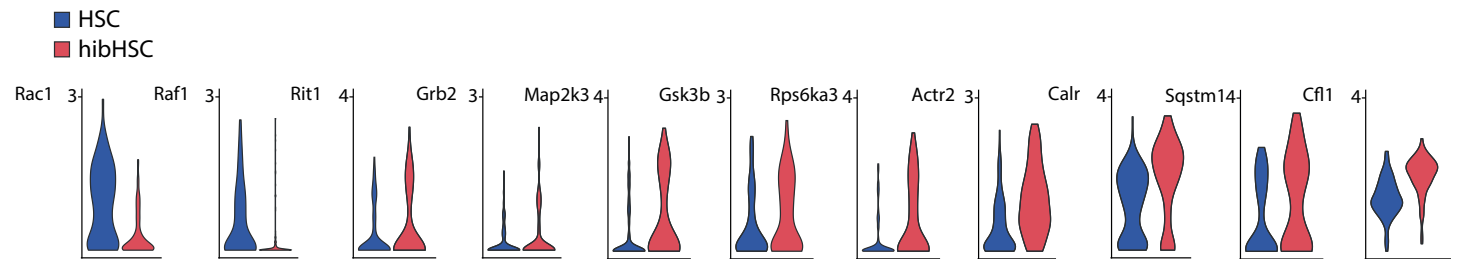
B



C



D



E

